Toward a universal model for spatially structured populations

Loïc Marrec[1 ¤a], Irene Lamberti[1 ¤b], Anne-Florence Bitbol[1,2 *]

1 Sorbonne Université, CNRS, Institut de Biologie Paris-Seine, Laboratoire Jean Perrin (UMR 8237), F-75005 Paris, France
2 Institute of Bioengineering, School of Life Sciences, École Polytechnique Fédérale de Lausanne (EPFL), CH-1015 Lausanne, Switzerland

¤a Current address: Institute of Ecology and Evolution, University of Bern, Baltzerstrasse 6, CH-3012 Bern, Switzerland
¤b Current address: Institute of Bioengineering, School of Life Sciences, École Polytechnique Fédérale de Lausanne (EPFL), CH-1015 Lausanne, Switzerland
* anne-florence.bitbol@epfl.ch

Abstract

Microbial populations often have complex spatial structures, with homogeneous competition holding only at a local scale. Population structure can strongly impact evolution, in particular by affecting the fixation probability of mutants. Here, we propose a model of structured microbial populations on graphs, where each node of the graph contains a well-mixed deme whose size can fluctuate, and where migrations are independent from birth and death events. We study analytically and numerically the mutant fixation probabilities in different structures, in the rare migration regime. In particular, we demonstrate that the star graph continuously transitions between amplifying and suppressing natural selection as migration rate asymmetry is varied. This elucidates the apparent paradox in existing constant-size models on graphs, where the star is an amplifier or a suppressor depending on the details of the dynamics or update rule chosen, e.g. whether each birth event precedes or follows a death event. The celebrated amplification property of the star graph for large populations is preserved in our model, for specific migration asymmetry. We further demonstrate a general mapping between our model and constant-size models on graphs, under a constraint on migration rates, which directly stems from assuming constant size. By lifting this constraint, our model reconciles and generalizes previous results, showing that migration rate asymmetry is key to determining whether a given population structure amplifies or suppresses natural selection.

Summary

A key question in evolution is how likely a mutant is to take over. This depends on natural selection and on stochastic fluctuations. Compared to a well-mixed population, some spatial structures have been predicted to amplify or suppress the impact of natural selection. This can have a major impact on evolution, as well as applications in biotechnology, e.g. by facilitating selection in directed evolution of biomolecules. We introduce a model for complex structured populations that generalizes over existing ones by allowing population size to fluctuate. We demonstrate that whether a given population structure amplifies or suppresses selection strongly depends on the asymmetry of migration rates. Our results are universal in the sense that they do not depend on update rules.

Introduction

Classical models of homogeneous and well-mixed microbial populations may give a good description of their evolution in a well-agitated liquid suspension, but of few natural situations. For instance, during an infection, microbial populations are subdivided between different organs [1, 2], and between different hosts. More generally, any spatial structure of a population implies a stronger competition between neighbors than between distant individuals, even for microorganisms growing on a Petri dish.

Population structure can have major consequences on the way microbial populations evolve. Remarkably, the fixation probability of a mutant in an asexual microbial population can be affected by population structure, with specific structures amplifying or suppressing natural selection [3]. Studying these effects requires going beyond simple population structures [4, 5] where migration is symmetric between demes (i.e. subpopulations), since fixation probabilities are unaffected in these cases [6, 7], unless extinctions of demes occur [8]. Ref. [3] introduced a seminal model for complex population structures, known as evolutionary dynamics on graphs, with one individual placed at each node of a graph, and probabilities that the offspring of an individual replaces another individual along each edge of the graph. However, in such models, evolutionary outcomes can drastically depend on the details of the dynamics or update rule, e.g. whether each birth event precedes a death event or the opposite [9–11]. This lack of universality raises issues for applicability to real microbial populations, where the order of birth and death is generally not fixed. Furthermore, in most microbial populations, individuals freely compete with their closest neighbors, thus motivating a coarse-graining of the description [3], with demes on graphs rather than individuals [4, 5, 12–15].

Here, we propose a model for complex population structures where each node of a graph contains a well-mixed deme whose size can fluctuate, and where migrations are independent from birth and death events. This frees us from the necessity of setting the order of events, in contrast to previous models [3, 13]. Focusing on rare migrations, we obtain analytical results in different population structures, which are compared to stochastic simulations. Within this new universal model of subdivided populations, we investigate the fixation probability of mutants, and find that both amplification and suppression of natural selection can occur, with strong dependence on the asymmetry of migration rates. We generalize the circulation theorem [3] to our model, thereby providing a criterion for structured populations to feature similar fixation probabilities as well-mixed ones. We relate and compare our model to existing ones [3, 13], finding a mapping to that of Ref. [3] under specific constraints on migration rates.

Model and methods

We model a structured population with D well-mixed demes as a directed graph where each node $i \in \{1, \ldots, D\}$ represents a deme with carrying capacity K_i, and migration rates m_{ij} per individual from deme i to deme $j \neq i$ are specified along each edge ij. We consider wild-type (W) and mutant (M) microorganisms, with fitnesses and death rates denoted by f_α and g_α, respectively, where $\alpha = W$ or $\alpha = M$. Their division rate in deme i is given by the logistic function $f_\alpha(1 - N_i/K_i)$, where N_i is the number of individuals present in deme i. We take $f_W = 1$, which amounts to considering the wild-type fitness as a reference. We address selection on birth, and hence assume $g_M = g_W$, but our results can be generalized to include selection on death. We focus on the regime where deme sizes N_i fluctuate weakly around their deterministic steady-state values.

We inquire about the fate of a mutant arising in a structured population: does it take over, i.e. fix, or does it go extinct? We assume that mutations are rare enough for further mutation events to be neglected while the fate of a given mutant lineage is determined, and thus we do not model mutation events. We consider that the initial mutant is placed randomly with a probability proportional to deme size, which is realistic for spontaneous mutations occurring upon division, or simply with a constant rate per individual (in the language of models with one individual per deme, this corresponds to uniform and temperature initial conditions [16], which coincide in our model). Under this initialization, the fixation probability of a neutral mutant is independent of population structure, as long as the underlying graph is not disconnected (see Supporting Information, section 1). Compared to the well-mixed population with the same total size, an *amplifier* of natural selection features a larger fixation probability for beneficial mutants, and a smaller one for deleterious mutants, while a *suppressor* has the opposite characteristics [17]. Furthermore, we focus on the rare migration regime, where fixation of a type (W or M) in a deme is much faster than migration timescales. Then, the state of the subdivided population can be described in a coarse-grained way by whether each deme is mutant or wild-type. Its evolution can be described as a Markov process where elementary steps are migration events, which change the state of the system if fixation ensues. This description allows us to obtain complete analytical results for fixation probabilities in graphs with strong symmetries (see Supporting Information, Section 2). In this regime, if one starts from a single mutant in deme i, this mutant first needs to fix in deme i before it can spread to other demes. Since fixation in a homogeneous deme is well-known,

we concentrate our efforts on the second stage of the process. Therefore, we ask whether the mutant fixes when starting from one fully mutant deme, while all others are fully wild-type. Our stochastic simulations, performed using a Gillespie algorithm (see Supporting Information, Section 8), allow us to test our analytical predictions.

Specifically, we investigate the fate of mutants in the structures shown in Fig 1.

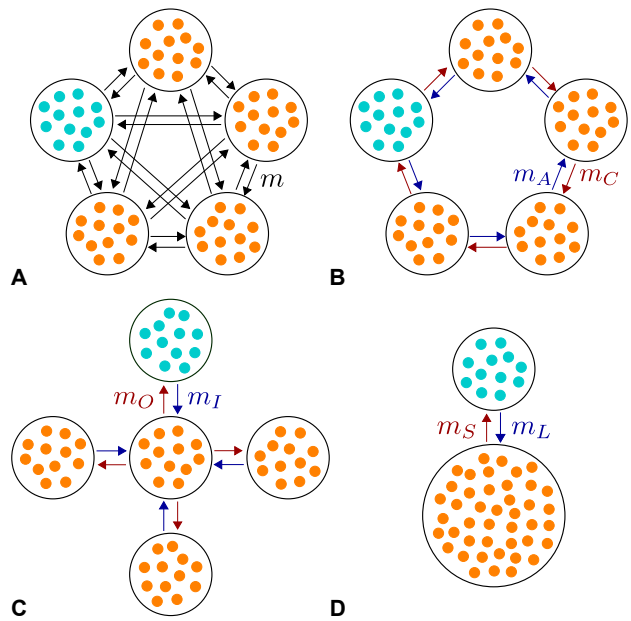

Fig 1. Some population structures. A: Clique. **B:** Cycle. **C:** Star. **D:** Doublet comprising a small deme and a larger deme. Mutants (M) are in blue, wild-type (W) in orange, and the state where the mutant type has fixed in one deme while all other demes are fully wild-type is represented. Arrows indicate migrations, with the associated rates per individual.

Results

Fixation of mutants on graphs with strong symmetries

We start by considering subdivided populations with D demes of identical carrying capacity K on graphs with strong symmetries, represented in Fig 1A, B and C.

Clique. The graph with full symmetry is the clique, or complete graph, where all demes are connected to all others with identical migration rates m per individual along each edge (Fig. 1A). Starting from one fully mutant deme and $D-1$ fully wild-type demes, the fixation probability Φ_1^{clique} of the mutant type in the clique reads (see Supporting Information, Section 2.1, for a derivation inspired by Ref. [18]):

$$\Phi_1^{\text{clique}} = \frac{1-\gamma}{1-\gamma^D} \,, \tag{1}$$

with

$$\gamma = \frac{N_W \rho_W}{N_M \rho_M} \,, \tag{2}$$

where N_W (resp. N_M) is the deterministic steady-state size of a wild-type (resp. mutant) deme and ρ_W (resp. ρ_M) is the fixation probability of a wild-type (resp. mutant) microbe in a mutant (resp. wild-type) deme. The fixation probability Φ_1^{clique}, which does not depend on migration rate m, is plotted versus mutant fitness in Fig. 2A, showing excellent agreement between Eq. 1 and our stochastic simulation results. Moreover, the fixation probability is very close to that in a well-mixed population with the same total size $N_W D$ starting from the same number N_W of mutants. In the Supporting Information, Section 2.1, we show that the clique is in fact a slight suppressor of selection for small mutational effects and high degrees of subdivision, but that specializing to a model where migrations are exchanges of individuals and assuming $N_M = N_W$ suppresses this effect. Importantly, Eq. 1 has the

exact same form as the fixation probability of a single mutant in a well-mixed population of fixed size D in the Moran model [19, 20], but with γ in Eq. 2 playing the role of the ratio f_W/f_M.

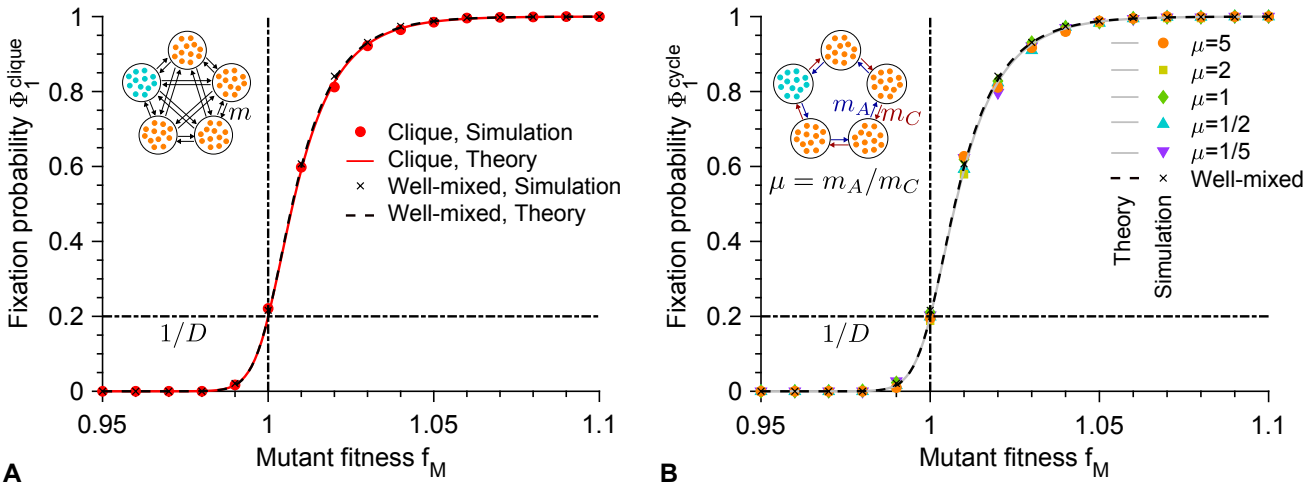

Fig 2. Fixation probabilities for the clique and for the cycle. The fixation probability Φ_1 of the mutant starting with one fully mutant deme chosen uniformly at random is shown versus mutant fitness f_M, for the clique in panel **A** and for the cycle in panel **B**, with different migration rate asymmetries $\mu = m_A/m_C$. Data for the well-mixed population is shown as reference, with same total population size and initial number of mutants. Markers are computed over 10^3 stochastic simulation realizations. Curves represent analytical predictions, Eq. 1 for the cycle and the clique, and Eq. S15 for the well-mixed population [19, 20]. Vertical dash-dotted lines indicate the neutral case $f_M = f_W$, and horizontal dash-dotted lines represent the neutral fixation probability. Parameter values: $D = 5$, $K = 100$, $f_W = 1$, $g_W = g_M = 0.1$ in both panels. In panel **A**, $m = 10^{-6}$ in simulations. In panel **B**, from top to bottom, $(m_A, m_C) \times 10^6 = (1, 5)$; $(1, 2)$; $(1, 1)$; $(2, 1)$; $(5, 1)$ in simulations.

Cycle. Another graph where all demes are equivalent is the cycle (see Fig. 1B). Clockwise and anti-clockwise migrations can have different rates per individual, denoted respectively by m_C and m_A. Exactly as for the clique, the fixation probability Φ_1^{cycle} of a mutation satisfies Eq. 1, which is independent on migration rates (see Supporting Information, Section 2.2). This is corroborated by our simulations, as shown in Fig. 2B.

Star. In the star graph, a central node is connected to all others, called leaves, while each leaf is only connected to the center (see Fig. 1C): all leaves are equivalent, but the center is different. An individual can migrate from a given leaf to the center with migration rate m_I and from the center to a given leaf with migration rate m_O. The fixation probability of the mutant type can be expressed exactly as a function of D, $\mu = m_I/m_O$ and γ defined in Eq. 2 (see Supporting Information, Section 2.3, for a derivation inspired by Ref. [21]):

$$\Phi_1^{\text{star}} = \frac{(1-\gamma^2)\left[\gamma + \mu D + \gamma\mu^2(D-1)\right]}{D\,(\mu+\gamma)\left[1 + \mu\gamma - \gamma^D(\mu+\gamma)^{2-D}\,(1+\mu\gamma)^{D-1}\right]}\,. \tag{3}$$

Fig. 3A shows the fixation probability Φ_1^{star} of the mutant in the star graph for different values of migration asymmetry $\mu = m_I/m_O$, with very good agreement between our analytical predictions and our numerical simulations (see also Fig. S1 for additional μ values and a heatmap). For $\mu = 1$, Φ_1^{star} is very close to the case of a well-mixed population. Indeed, we show in the Supporting Information, Section 2.3, that it then reduces to that of the clique, Eq. 1. Furthermore, if $\mu < 1$, the star is a suppressor of selection compared to the clique, while for $\mu > 1$ it is an amplifier of selection at least in some range of mutant fitnesses f_M (see Supporting Information, Section 2.3). For $\mu = D - 1$, our fixation probability has the exact same form [21] as that of a single mutant in a star of D single individuals in the model of Ref. [3], but with γ defined in Eq. 2 playing the role of f_W/f_M. The celebrated universal amplification property of the star in the large D limit [22] is thus exactly recovered in our model for $\mu = D - 1$, but more generally, we find amplification for $\mu > 1$, and suppression for $\mu < 1$ (see Fig. 3B). Qualitatively, for large D, mutants very likely start in a leaf. If μ is large, the center is often invaded, which helps fit mutants take over.

Conversely, if μ is small, the center often invades the leaves, thus preventing any mutant originating in a leaf from fixing.

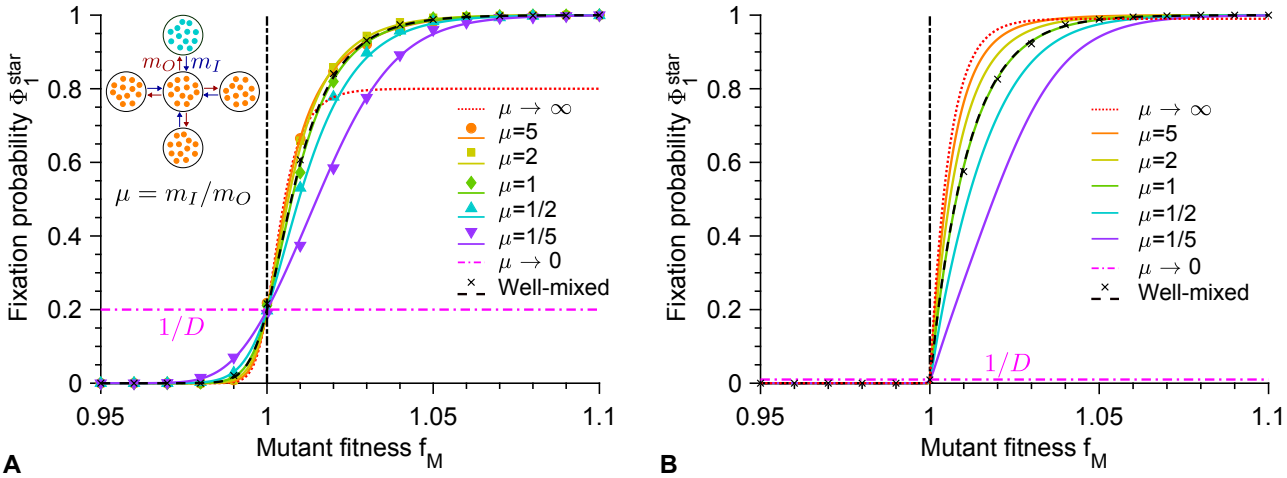

Fig 3. Fixation probability for the star. Fixation probability Φ_1^{star} of a mutant in a star graph versus mutant fitness f_M, starting with one fully mutant deme chosen uniformly at random, for different migration rate asymmetries $\mu = m_I/m_O$. Number of demes: $D = 5$ in panel **A**, $D = 100$ in panel **B**. Data for the well-mixed population is shown as reference, with same total population size and initial number of mutants. Markers are computed over 2×10^3 stochastic simulation realizations. Curves represent analytical predictions in Eq. 3. Vertical dash-dotted lines indicate the neutral case $f_W = f_M$. Parameter values: $K = 100$, $f_W = 1$, $g_W = g_M = 0.1$. In panel **A**, from top to bottom, $(m_I, m_O) \times 10^6 = (5, 1)$; $(2, 1)$; $(1, 1)$; $(1, 2)$; $(1, 5)$ in simulations.

Comparison with existing models

Ref. [3] introduced a seminal model of subdivided populations on graphs, where each node of the graph is occupied by a single individual. An exact mapping can be made between the model of Ref. [3] and our model, if the same graph is considered for both models, with one individual per node in the first case and with a deme of carrying capacity K per node in the second one (see Supporting Information, Section 3). Specifically, the probability that, upon a division, the offspring from node i replaces the individual on node j in the model of Ref. [3] maps to the probability that, upon a migration event resulting into fixation, an individual from deme i fixes in deme j in our model. In this mapping, which holds for all graphs, the product of deme size and fixation probability in a deme in our model plays the part of fitness in the model of Ref. [3]. However, an important constraint in the "Birth-death" model of Ref. [3] is that migration probabilities w_{ij} between demes satisfy $\sum_j w_{ij} = 1$ for all i, while migration rates m_{ij} in our model are all independent. Our model is thus less constrained, and generalizes and coarse-grains that of Ref. [3].

For the clique and for the cycle, we found that the fixation probability starting from one mutant deme (Eq. 1) has the same form as that for a well-mixed population starting with one mutant individual, but with $\gamma = N_W \rho_W/(N_M \rho_M)$ playing the part of f_W/f_M. For the star, we found that, if $\mu = D - 1$, our results have the exact same form as in the model of Ref. [3], again with γ playing the part of f_W/f_M. These results are perfectly consistent with the general mapping where $N\rho$ in our model plays the part of f in that of Ref. [3]. Furthermore, for the star, the equivalence is restricted to the specific case where $\mu = D - 1$, which is a direct consequence of the constraint $\sum_j w_{ij} = 1$ for all i (see Supporting Information, Section 3).

While the star is a universal amplifier for large D in the model of Ref. [3], it can be either a suppressor or an amplifier of selection, depending on μ, in our model. This is because the number D of demes and the migration asymmetry $\mu = m_I/m_O$ are two independent parameters. Fig. 4 shows that restricting to the line $\mu = D - 1$ in our model yields amplification, while suppression occurs for smaller values of μ. In models with one individual per node, the star is an amplifier of selection in the large D limit for the Birth-death dynamics ("update rule"), where one individual is chosen to divide and its offspring replaces one of its neighbors on the graph [3], but a suppressor for the death-Birth dynamics, where one individual is chosen to die and is replaced by the offspring of one of its neighbors (selection being on division rates in both cases, which we indicate by the uppercase "Birth" [10]) [10, 17, 23, 24].

Consistently, the latter dynamics would yield $\mu = 1/(D-1)$. Our model shows that the impact of a given graph on selection fundamentally depends on migration asymmetry, rather than on the details of the chosen dynamics.

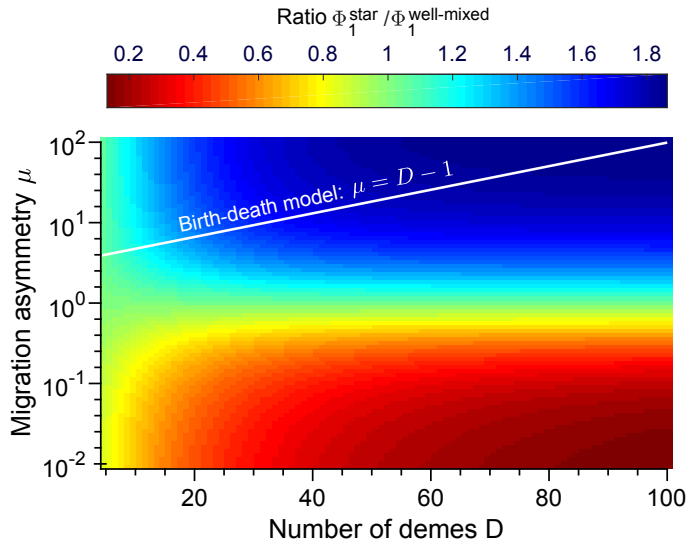

Fig 4. Amplification and suppression properties for the star. Heatmap of the ratio of the fixation probability Φ_1^{star} of the mutant type in a star graph to that $\Phi_1^{\text{well-mixed}}$ in a well-mixed population with same total population size and initial number of mutants, versus number D of demes and migration rate asymmetry $\mu = m_I/m_O$. The star is initialized with one fully mutant deme chosen uniformly at random. Data from analytical formula in Eq. 3 for the star, and in Eq. S15 for the well-mixed population. Parameter values: $K = 100$, $f_W = 1$, $f_M = 1.001$, $g_W = g_M = 0.1$.

In line with the mapping between our model and that of Ref. [3], a generalized circulation theorem holds for our model (see Supporting Information, section 4), in the spirit of Ref. [3]. Specifically, a population of D demes on a graph has the same mutant fixation probability as the clique with the same size if and only if, for all nodes of the graph, the total rate of migrations leaving a node is equal to the total rate of migrations arriving in this node. Among the structures we considered, in addition to the clique, the cycle is a circulation, which explains why we found the same fixation probability in the cycle as in the clique, for any migration asymmetry.

Ref. [13] introduced a model generalizing that of Ref. [3] to the case where each node of the graph is occupied by a deme with fixed population size (see also Refs. [12, 15, 25] for related models). In this model, as in Ref. [3], each elementary event is composed of a birth in one deme and a death in another one, yielding Birth-death and death-Birth models that give different results. The regime of rare migrations in our model corresponds to strong self-loops (migrations to the same deme) in the model of Ref. [13]. For the star with self-loops [16], we show in the Supporting Information, section 5 that by matching migration-to-division rate ratios in each deme, both models yield similar simulation results. However, even in that case, a difference is that death rate (resp. birth rate) is not homogeneous across demes in the Birth-death (resp. death-Birth) models of Ref. [13], unless migrations are symmetric. In our model, migration, death and birth events are all independent, allowing us to remove such artificial constraints.

Extension to different deme sizes: the doublet

Our model allows us to consider structures involving demes with different sizes. As a simple example, consider a doublet comprising a small deme with carrying capacity K_S and a larger deme with carrying capacity $K_L > K_S$ (see Fig. 1D). Individuals can migrate from the large (resp. small) deme to the small (resp. large) deme with a rate per individual m_S (resp. m_L). For structured populations involving demes with identical sizes, we considered the fixation probability Φ_1 starting from one fully mutant deme, which yields that of one mutant individual when multiplied by ρ_M. Here, we consider the fixation probability of one single mutant in the structure divided by that in the small deme. If $K_L = (D-1)K_S$ and $K_S = K$, this quantity Φ_1^{doublet} is analogous to our usual Φ_1, thus facilitating comparisons. Φ_1^{doublet} is expressed analytically in the Supporting Information, Section 6.

Fig. 5 shows Φ_1^{doublet} for different migration asymmetries $\mu = m_S/m_L$, with excellent agreement between our analytical predictions and our simulation results (see also Fig. S4 for additional μ values and a heatmap).

Furthermore, Fig. 5 shows that the fixation probability is very close to the well-mixed case when $\mu = 1/(D-1)$. This corresponds to $m_S K_L = m_L K_S$, i.e. to equal migration flows from small to large deme and reciprocally. We also observe that the doublet behaves as a suppressor of selection for $\mu > 1/(D-1)$, and has weak amplifying properties for $\mu < 1/(D-1)$, which do not survive in the limit $\mu \to 0$. In the Supporting Information, Section 6, we show that in the regime of moderate mutational effects, the doublet is an amplifier of selection with respect to the clique for $1/(D-1)^2 < \mu < 1/(D-1)$, and a suppressor of selection for $\mu > 1/(D-1)$. This generalizes the result of Ref. [3] that small upstream populations with large downstream populations, corresponding here to $\mu \to 0$, yield suppressors. Furthermore, this confirms the importance of migration asymmetry in the impact a population structure has on selection.

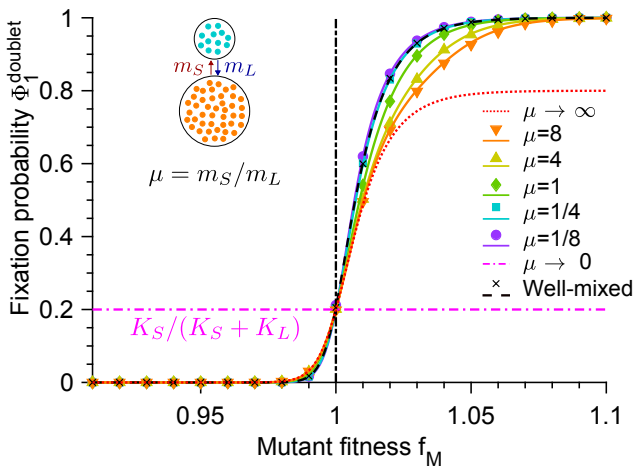

Fig 5. Fixation probability for the doublet. Fixation probability Φ_1^{doublet} of a mutant in a doublet versus mutant fitness f_M, starting with one fully mutant deme chosen proportionally to deme size, with different migration asymmetries $\mu = m_S/m_L$. Data for the well-mixed population is shown as reference, with same total population size and initial number of mutants. Markers are computed over 2×10^3 stochastic simulation realizations. Curves represent analytical predictions in Eqs. S84, S85 and S87. Vertical dash-dotted lines indicate the neutral case $f_W = f_M$. Parameter values: $K_S = 100$, $K_L = 400$ (hence $K_L = (D-1)K_S$ with $K_S = K = 100$ and $D = 5$), $f_W = 1$, $g_W = g_M = 0.1$. From top to bottom, $(m_S, m_L) \times 10^6 = (8,1)$; $(4,1)$; $(1,1)$; $(1,4)$; $(1,8)$ in simulations.

Discussion

We developed a model of structured microbial populations on graphs, with demes whose size can fluctuate around a steady-state value. Compared to existing models [3, 13], lifting the constraint of constant population size allowed us to treat migration, birth and death as independent events. For rare migrations and graphs with strong symmetries, we gave analytical expressions of mutant fixation probabilities. In particular, we demonstrated that the star graph continuously transitions between amplifying and suppressing natural selection as migration rate asymmetry is varied. This elucidates the apparent paradox in constant-size models, where the star, like many random graphs [10], is an amplifier in the Birth-death dynamics and a suppressor in the death-Birth dynamics [10, 17, 23, 24]. Furthermore, we found a mapping between our model and the seminal model of Ref. [3], under a constraint on migration rates. Constant size models require making specific choice on the dynamics ("update rule"), which constrain migration rates. By lifting this constraint, our model reconciles and generalizes the results obtained in these different dynamics, showing that migration rate asymmetry is key to determining whether a given population structure amplifies or suppresses natural selection. Our model also applies to populations with different deme sizes, where the impact of migration asymmetry is also crucial.

Birth-death dynamics may be realistic for extreme resource limitation, such that one birth causes one death, while death-Birth dynamics may better model cases where death frees resources, e.g. light for plants [23, 26]. However, in general, in a microbial population, population size is not exactly fixed and the order of birth and death events is not set. Thus, our more universal model, where results do not depend on update rules, should apply more generally. The differences between Birth-death and death-Birth dynamics are major for mutant fixation probabilities, but also in evolutionary game theory, where spatial structure can promote the evolution of cooperation in the latter case, but

not in the former [27–29]. Previous efforts were made to generalize beyond these dynamics by allowing both types of update to occur in given proportions [30, 31]. Interestingly, it was recently shown that no strong or universal amplification of selection can occur when even a small proportion of death-Birth events occurs [31], in contrast to the Birth-death case. Conversely, in our model, the universal amplification property of the star graph in the large-size limit is fully preserved, for sufficient migration asymmetry.

While our focus was on mutant fixation probabilities, our model can be employed to investigate fixation times and evolution rate [15, 32–38]. It can also address more complex population structures [17, 39], e.g. motivated by within-host or between-host pathogen dynamics [40]. Our model can be extended in multiple ways, in particular beyond the regime of rare migrations, and to models of evolutionary game theory. Finally, it opens the way to experimental tests in quantitative evolution experiments, e.g. in microfluidic devices allowing to control flow between different populations [41], and to applications in biotechnology, e.g. by allowing to amplify *in vivo* selection in the directed evolution of biomolecules [42].

Acknowledgments

This project has received funding from the European Research Council (ERC) under the European Union's Horizon 2020 research and innovation programme (grant agreement No. 851173, to AFB). LM acknowledges funding by a graduate fellowship from EDPIF. LM thanks his grandfather, Jean Polard, for inspiration.

Supporting Information

Contents

1 Fixation probability of neutral mutants **10**

2 Fixation probabilities in strongly symmetric graphs **10**
2.1 Clique 10
2.2 Cycle 13
2.3 Star 13

3 Comparison with the model of Ref. [3] **17**

4 Generalized circulation theorem **18**

5 Comparison with the model of Ref. [13] **20**

6 A simple structure with different population sizes: the doublet **24**

7 Constant deme size approximation **26**

8 Simulation methods **28**

1 Fixation probability of neutral mutants

Consider a graph made of nodes i, each associated to a deme with steady-state population size N_i, and edges ij where migration rates m_{ij} from deme i to deme j are specified. Further assume that the graph is not disconnected. Consider uniform initial conditions: a mutant has probability $N_i/\sum_j N_j$ to be initially placed in deme i. A neutral mutant then has probability $1/N_i$ to fix in deme i (taking the result for constant population size [20]). Let $\Phi_1^{(i)}$ denote the probability that the mutant fixes in the whole metapopulation, starting from a fully mutant deme i, all other demes being fully wild-type. The overall fixation probability of one mutant in the metapopulation reads

$$\rho_M = \sum_i \frac{N_i}{\sum_j N_j} \frac{1}{N_i} \Phi_1^{(i)} = \frac{\sum_i \Phi_1^{(i)}}{\sum_i N_i} \,. \tag{S1}$$

Let us now remark that, because the graph is not disconnected, after a sufficient time, all individuals in the metapopulation are descended from the same deme. If we start from one deme i that is fully mutant and all others that are fully wild-type, this yields

$$\Phi_1^{(i)} + \sum_{j \neq i} \Psi_1^{(j)} = 1 \,, \tag{S2}$$

where $\Psi_1^{(j)}$ is the probability that wild-type individuals from deme j fix in the whole metapopulation. But since the mutant is assumed to be neutral, we have $\Psi_1^{(j)} = \Phi_1^{(j)}$, and thus Eq. S2 becomes

$$\sum_i \Phi_1^{(i)} = 1 \,. \tag{S3}$$

Therefore, combining Eqs. S1 and S3, we obtain

$$\rho_M = \frac{1}{\sum_i N_i} \,, \tag{S4}$$

which is exactly the fixation probability of one neutral mutant in a well-mixed population of size $\sum_i N_i$ [20]. Thus, provided that the graph is not disconnected, the fixation probability of a neutral mutant under uniform initial conditions is independent of population structure in our model.

In the particular case where all D demes have the same size, i.e. $N_i \equiv N$ does not depend on i, then $\rho_M = 1/(ND)$, and the average fixation probability starting from one single fully mutant deme under uniform initial conditions is

$$\Phi_1 = \sum_i \frac{N_i}{\sum_j N_j} \Phi_1^{(i)} = \frac{\sum_i \Phi_1^{(i)}}{D} = \frac{1}{D} \,. \tag{S5}$$

2 Fixation probabilities in strongly symmetric graphs

2.1 Clique

Let us consider a population with D demes, structured as a clique, i.e. where migration rates per individual between all demes are equally likely. The state of the system can be fully described by the number i of mutant demes. We denote by m the migration rate per individual from one deme to any other deme. Recall that in our model, migration occur between two different demes (no migration can end in the deme where it started). Let us assume that we start from i fully mutant demes and $D-i$ fully wild-type demes. Recall that the wild-type is denoted by W and the mutant by M.

Consider the outcome of a migration event. The number of mutant demes increases by 1 if an M individual migrates from one of the i mutant demes to one of the $D-i$ wild-type demes, and fixes there. The probability that this occurs upon a migration event thus reads

$$T_i^+ = \frac{mN_M i}{mN_M i + mN_W(D-i)} \frac{D-i}{D-1} \rho_M = \frac{N_M i}{N_M i + N_W(D-i)} \frac{D-i}{D-1} \rho_M \,, \tag{S6}$$

where

$$\rho_M = \frac{1-r}{1-r^{N_W}} \tag{S7}$$

is the fixation probability of a mutant microbe in a wild-type deme in the Moran process [19, 20] (see section 7) where

$$r = \frac{f_W}{f_M} \,, \tag{S8}$$

and $N_W = K(1 - g_W/f_W)$ is the steady-state size of a wild-type deme. Similarly, the number of mutant demes decreases by 1 if a W individual migrates from one of the $D - i$ wild-type demes to one of the i mutant demes, and fixes there. The probability that this occurs upon a migration event thus reads

$$T_i^- = \frac{N_W(D-i)}{N_M i + N_W(D-i)} \, \frac{i}{D-1} \, \rho_W \,, \tag{S9}$$

where

$$\rho_W = \frac{1 - r^{-1}}{1 - r^{-N_M}} \tag{S10}$$

is the fixation probability of a wild-type microbe in a mutant deme, with r in Eq. S8, and $N_M = K(1 - g_M/f_M)$ is the steady-state size of a mutant deme.

The fixation probability Φ_i^{clique} of the mutant type in a clique of D demes starting with i fully mutant demes satisfies the recurrence relation

$$\begin{cases} \Phi_0^{\text{clique}} = 0 \\ \Phi_i^{\text{clique}} = T_i^+ \Phi_{i+1}^{\text{clique}} + T_i^- \Phi_{i-1}^{\text{clique}} + (1 - T_i^+ - T_i^-)\Phi_i^{\text{clique}} \text{ for } 1 \le i \le D-1 \\ \Phi_D^{\text{clique}} = 1 \,, \end{cases} \tag{S11}$$

where the second equation follows from distinguishing the different outcomes of the first migration event. Eq. S11 can be solved e.g. as in Ref. [18], yielding

$$\Phi_i^{\text{clique}} = \frac{1 + \sum_{k=1}^{i-1} \prod_{j=1}^{k} \gamma_j}{1 + \sum_{k=1}^{D-1} \prod_{j=1}^{k} \gamma_j} \,, \tag{S12}$$

where $\gamma_i = T_i^-/T_i^+ = N_W \rho_W / (N_M \rho_M)$. Since here γ_i does not depend on the initial number i of mutant demes, the fixation probability Φ_i^{clique} reduces to

$$\Phi_i^{\text{clique}} = \frac{1 - \gamma^i}{1 - \gamma^D} \,, \tag{S13}$$

with

$$\gamma = \frac{N_W \rho_W}{N_M \rho_M} \,. \tag{S14}$$

Note that in the neutral case where $\gamma = 1$, Eq. S12 yields $\Phi_i^{\text{clique}} = i/D$, consistently with Eq. S5.

Eq. S13 has the same form as the fixation probability of i mutants in a well-mixed population of N individuals in the Moran model [19, 20], namely

$$\rho_i = \frac{1 - r^i}{1 - r^N} \,, \tag{S15}$$

with r in Eq. S8 (note that Eq. S7 corresponds to the case $i = 1$). Specifically, Eq. S15 maps to Eq. S13 by replacing N with D and r with γ. Thus, the clique can be thought of a coarse-grained version of the well-mixed population: each deme is identically connected to all other demes, just like all individuals are in competition in the well-mixed population.

To obtain the fixation probability ρ_M^{clique} of a single mutant individual in the clique, one needs to include the fixation of the mutant in one deme before the spread from that deme to the full metapopulation. Thus, it reads

$$\rho_M^{\text{clique}} = \rho_M \Phi_1^{\text{clique}} \,, \tag{S16}$$

with ρ_M given by Eq. S7 and Φ_1^{clique} by Eq. S13 for $i = 1$.

Expansion for very small mutational effects. Let ϵ be such that $f_M = f_W(1+\epsilon)$. Consider the regime where $\epsilon \ll 1$ and $N_W|\epsilon| \ll 1$. Then Eq. S13 gives (for $i = 1$)

$$\Phi_1^{\text{clique}} = \frac{1}{D}\left[1 + \frac{\epsilon}{2}(D-1)\left(N_W - 1 + \frac{2g}{f_W - g}\right) + O(\epsilon^2)\right] . \tag{S17}$$

Eqs. S15 and S16 then allow us to show that

$$\frac{\rho_M^{\text{clique}}}{\rho_M^{\text{well-mixed}}} = 1 - \frac{\epsilon}{2}(D-1)\left(1 - \frac{2g}{f_W - g}\right) + O(\epsilon^2) , \tag{S18}$$

where $\rho_M^{\text{well-mixed}}$ is the fixation probability of a mutant in a well-mixed population with $N_W D$ individuals. Therefore, the clique is a suppressor of natural selection in this regime if $g < f/3$. Suppression is all the more important that the degree of subdivision is high, namely the number D of demes (recall that here we compare a clique and a well-mixed population for the same total population size $N_W D$).

Expansion for relatively small mutational effects. Next, consider the regime where $\epsilon \ll 1$ and $N_W|\epsilon| \gg 1$ but $N_W\epsilon^2 \ll 1$. Then, if $\epsilon > 0$,

$$\Phi_1^{\text{clique}} = 1 - e^{-N_W\epsilon}\left[1 + O(\epsilon) + O(N_W\epsilon^2)\right] , \tag{S19}$$

which means that fixation is almost certain (recall that if one starts from one single mutant, this holds provided that a mutant has fixed in a deme, which occurs with probability $\rho_M = \epsilon + O(\epsilon^2)$, see Eq. S7). Therefore, Eq. S16 yields $\rho_1^{\text{clique}} = \epsilon + O(\epsilon^2)$, which is equal (to this order) to the fixation probability $\rho_{1,N_W D}^{\text{well-mixed}}$ in a well-mixed population with the same total size $N_W D$. Now, if $\epsilon < 0$,

$$\Phi_1^{\text{clique}} = e^{N_W(D-1)\epsilon}\left[1 + O(\epsilon) + O(N_W\epsilon^2)\right] . \tag{S20}$$

which means that fixation is exponentially suppressed. Thus, Eq. S16 yields $\rho_1^{\text{clique}} = e^{N_W D\epsilon}\left[1 + O(\epsilon) + O(N_W\epsilon^2)\right]$, which is equal (to this order) to the fixation probability $\rho_1^{\text{well-mixed}}$ in a well-mixed population with the same total size $N_W D$. Hence, in this regime, the fixation probability of a mutant in the clique is very close to that in a well-mixed population with the same total size $N_W D$, and the suppression effect found for extremely small mutational effects is quite restricted.

Model specialized to symmetric migrations. In the clique, migrations are symmetric, i.e. $m_{ij} = m_{ji} = m$ for all $i \neq j$. Let us consider another model, restricted to symmetric migrations, where each migration event is modeled as an exchange between two individuals from two different demes. Let us further neglect the difference between N_M and N_W, and assume $N_M = N_W = N$. Upon a given migration event, the probability that the number i of mutant demes increases is

$$T_i^+ = \frac{2i(D-i)}{D(D-1)}\rho_M(1-\rho_W) , \tag{S21}$$

and similarly, the probability that i decreases is

$$T_i^- = \frac{2i(D-i)}{D(D-1)}\rho_W(1-\rho_M) , \tag{S22}$$

yielding as above the fixation probability Φ_1^{clique} in Eq. S13 when one starts from one mutant deme, but with

$$\gamma = \frac{\rho_W(1-\rho_M)}{\rho_M(1-\rho_W)} . \tag{S23}$$

Eq. S16 then yields the fixation probability of one single mutant

$$\rho_M^{\text{clique, sym}} = \rho_M \Phi_1^{\text{clique}} = \frac{1-r}{1-r^{ND}} , \tag{S24}$$

with r defined in Eq. S8. This is exactly the fixation probability of a mutant in a well-mixed population of fixed size ND in the Moran model (see above).

2.2 Cycle

Let us consider a population structured as a cycle with D demes, starting from exactly one fully mutant deme. During the fixation process, this will yield a cluster of i consecutive mutant demes that cannot break. Therefore, in this process, the state of the system can be fully described by the number i of (consecutive) mutant demes. Upon a migration event, the number i of mutant demes increases by 1 if a M individual from one of the two extremities of the mutant cluster migrates to the neighboring wild-type deme and fixes there. The probability that this occurs thus reads

$$T_i^+ = \frac{(m_C + m_A)N_M}{(m_C + m_A)N_M i + (m_C + m_A)N_W(D - i)}\,\rho_M\,, \tag{S25}$$

with ρ_M given by Eq. S7. Similarly, the number i of mutant demes decreases by 1 if a W individual from either of the two wild-type demes surrounding the mutant cluster migrates and fixes in its neighboring mutant deme. The probability that this occurs upon a migration event thus reads

$$T_i^- = \frac{(m_C + m_A)N_W}{(m_C + m_A)N_M i + (m_C + m_A)N_W(D - i)}\,\rho_W\,. \tag{S26}$$

Thus, the fixation probability Φ_i of mutation starting with i consecutive mutant demes satisfies Eq. S11 with T_i^+ and T_i^- given by Eqs. S25 and S26, which yields the fixation probability in Eq. S13 with γ given by Eq. S14. The fixation probability in the cycle, starting from exactly one fully mutant deme, is thus equal to that of the clique with the same number of demes.

2.3 Star

Let us consider a population structured as a star with D demes. Migrations from each single leaf to the center occur with a rate per individual m_I while migrations from the center to each single leaf occur with a migration rate per individual m_O. The state of the system can be fully described by a binary number indicating whether the center is wild-type or mutant and the number i of mutant leaves.

Upon a given migration event, the probability that the mutant type fixes in the center, if the center is initially wild-type and i leaves are mutant, reads

$$T_{(0,i)\to(1,i)} = \frac{m_I N_M i}{m_I N_M i + m_I N_W(D-1-i) + m_O N_W(D-1)}\rho_M\,, \tag{S27}$$

because it happens if migration occurs from a mutant leaf to the center, and the mutant then fixes in the center. Similarly, the probability that the wild-type fixes in the center, if the center is initially mutant and i leaves are mutant, reads

$$T_{(1,i)\to(0,i)} = \frac{m_I N_W(D-1-i)}{m_I N_M i + m_I N_W(D-1-i) + m_O N_W(D-1)}\rho_W\,, \tag{S28}$$

while the probability that the number of mutant leaves increases by 1 if the center is mutant is

$$T_{(1,i)\to(1,i+1)} = \frac{m_O N_M(D-1-i)}{m_I N_M i + m_I N_W(D-1-i) + m_O N_W(D-1)}\rho_M\,, \tag{S29}$$

and the probability that the number of mutant leaves decreases by 1 if the center is wild-type is

$$T_{(0,i)\to(0,i-1)} = \frac{m_O N_W i}{m_I N_M i + m_I N_W(D-1-i) + m_O N_W(D-1)}\rho_W\,. \tag{S30}$$

Let $\Phi_{0,i}^{\text{star}}$ be the fixation probability of the mutant type starting from i fully mutant leaves and a wild-type center. Similarly, let $\Phi_{1,i}^{\text{star}}$ be the fixation probability of the mutant type starting from i fully mutant leaves and a mutant center. The fixation probabilities $\Phi_{0,i}^{\text{star}}$ and $\Phi_{1,i}^{\text{star}}$ satisfy the following recurrence relationship, which is analogous to that in Ref. [21]:

$$\begin{cases} \Phi_{0,0}^{\text{star}} = 0\,, \\ \Phi_{1,i}^{\text{star}} = T_{(1,i)\to(0,i)}\Phi_{0,i}^{\text{star}} + T_{(1,i)\to(1,i+1)}\Phi_{1,i+1}^{\text{star}} \\ \qquad + \left[1 - T_{(1,i)\to(0,i)} - T_{(1,i)\to(1,i+1)}\right]\Phi_{1,i}^{\text{star}} \text{ for } 0 \le i \le D-2\,, \\ \Phi_{0,i}^{\text{star}} = T_{(0,i)\to(1,i)}\Phi_{1,i}^{\text{star}} + T_{(0,i)\to(0,i-1)}\Phi_{0,i-1}^{\text{star}} \\ \qquad + \left[1 - T_{(0,i)\to(1,i)} - T_{(0,i)\to(0,i-1)}\right]\Phi_{0,i}^{\text{star}} \text{ for } 1 \le i \le D-1\,, \\ \Phi_{1,D-1}^{\text{star}} = 1\,, \end{cases} \tag{S31}$$

Employing the expressions of the transition probabilities given above, the system S31 can be rewritten as:

$$\begin{cases} \Phi_{0,0}^{\text{star}} = 0\,, \\ \Phi_{1,i}^{\text{star}} = \Phi_{1,i-1}^{\text{star}} + \Gamma_1(\Phi_{1,i-1}^{\text{star}} - \Phi_{0,i-1}^{\text{star}}) \text{ for } 1 \le i \le D-1\,, \\ \Phi_{0,i}^{\text{star}} = \dfrac{1}{1+\Gamma_0}\Phi_{1,i}^{\text{star}} + \dfrac{\Gamma_0}{1+\Gamma_0}\Phi_{0,i-1}^{\text{star}} \text{ for } 1 \le i \le D-1\,, \\ \Phi_{1,D-1}^{\text{star}} = 1\ , \end{cases} \tag{S32}$$

where $\Gamma_1 = \gamma\, m_I/m_O$ and $\Gamma_0 = \gamma\, m_O/m_I$, with γ given in Eq. S14. Solving the system S32 yields

$$\begin{cases} \Phi_{0,0}^{\text{star}} = 0\,, \\ \Phi_{1,i}^{\text{star}} = \dfrac{-1+\Gamma_1\left[-1+(1+\Gamma_0)\left(\frac{\Gamma_0(1+\Gamma_1)}{1+\Gamma_0}\right)^i\right]}{-1+\Gamma_1\left[-1+(1+\Gamma_0)\left(\frac{\Gamma_0(1+\Gamma_1)}{1+\Gamma_0}\right)^{D-1}\right]} \text{ for } 0 \le i \le D-2\,, \\ \Phi_{0,i}^{\text{star}} = \dfrac{(1+\Gamma_1)\left[-1+\left(\frac{\Gamma_0(1+\Gamma_1)}{1+\Gamma_0}\right)^i\right]}{-1+\Gamma_1\left[-1+(1+\Gamma_0)\left(\frac{\Gamma_0(1+\Gamma_1)}{1+\Gamma_0}\right)^{D-1}\right]} \text{ for } 1 \le i \le D-1\,, \\ \Phi_{1,D-1}^{\text{star}} = 1\ . \end{cases} \tag{S33}$$

In particular, the fixation probability of the mutant type starting from one fully mutant center and all leaves fully wild-type reads

$$\Phi_{1,0}^{\text{star}} = \frac{1-\gamma^2}{1+\mu\gamma-\gamma(\mu+\gamma)\left(\frac{\gamma(1+\mu\gamma)}{\mu+\gamma}\right)^{D-1}}\ , \tag{S34}$$

where

$$\mu = \frac{m_I}{m_O}\,. \tag{S35}$$

The fixation probability of the mutant type starting from one fully mutant leaf and all other demes fully wild-type reads

$$\Phi_{0,1}^{\text{star}} = \frac{\frac{\mu}{\mu+\gamma}(1+\mu\gamma)\left(1-\gamma^2\right)}{1+\mu\gamma-\gamma(\mu+\gamma)\left(\frac{\gamma(1+\mu\gamma)}{\mu+\gamma}\right)^{D-1}} = \frac{\mu}{\mu+\gamma}(1+\mu\gamma)\Phi_{1,0}^{\text{star}}\ . \tag{S36}$$

The probability that the mutant type fixes, starting from a mutant deme that can be any deme of the star with equal probability, can then be expressed as

$$\begin{aligned} \Phi_1^{\text{star}} &= \frac{1}{D}\Phi_{1,0}^{\text{star}} + \frac{D-1}{D}\Phi_{0,1}^{\text{star}} = \frac{\gamma+\mu D+\gamma\mu^2(D-1)}{D\,(\mu+\gamma)}\Phi_{1,0}^{\text{star}} \\ &= \frac{\gamma+\mu D+\gamma\mu^2(D-1)}{D\,(\mu+\gamma)}\frac{1-\gamma^2}{1+\mu\gamma-\gamma(\mu+\gamma)\left(\frac{\gamma(1+\mu\gamma)}{\mu+\gamma}\right)^{D-1}}\ . \end{aligned} \tag{S37}$$

which can be rewritten as Eq. 3 in the main text.

Importantly, Eqs. S34, S36 and S37 are exactly equivalent to the formula given in Ref. [21] if the following substitutions are made: $\gamma \to f_W/f_M$ and $\mu \to D-1$ (bearing in mind that in the notations of Ref. [21], $D-1$ is called n and f_W/f_M is called $1/r$).

Expansion for very small mutational effects. Let ϵ be such that $f_M = f_W(1+\epsilon)$. For uniform initialization, consider the regime where $\epsilon \ll 1$ and $N_W|\epsilon| \ll 1$. Then Eq. S37 yields

$$\Phi_1^{\text{star}} = \frac{1}{D}\left[1+\epsilon\,\frac{\mu(D-1)\left[\mu(D-2)+2\right]}{(\mu+1)\left[\mu(D-1)+1\right]}\left(N_W-1+\frac{2g}{f-g}\right)+O(\epsilon^2)\right]\ . \tag{S38}$$

Comparing Eqs. S17 and S38 yields

$$\frac{\Phi_1^{\text{star}}}{\Phi_1^{\text{clique}}} = 1+\frac{\epsilon}{2}\left(N_W-1+\frac{2g}{f-g}\right)(D-1)\frac{(\mu-1)\left[\mu(D-3)+1\right]}{(\mu+1)\left[\mu(D-1)+1\right]}+O(\epsilon^2)\,. \tag{S39}$$

Assuming $D > 2$, the first-order term in Eq. S39 has the same sign as $\epsilon(\mu - 1)$. Thus, in this regime, the star is an amplifier of selection with respect to the clique for $\mu > 1$, and a suppressor for $\mu < 1$. Furthermore, for $D > 3$ (and integer), the function

$$F : \mu \mapsto \frac{(\mu - 1)\left[\mu(D-3)+1\right]}{(\mu + 1)\left[\mu(D-1)+1\right]}, \tag{S40}$$

increases with μ for $\mu > 0$, which entails that, for very small mutational effects, the strongest amplification is obtained for $\mu \gg 1$, where $F(\mu) \to 1$. Conversely, if $\mu \ll 1$ and $\mu \ll 1/D$, Eq. S38 yields

$$\Phi_1^{\text{star}} = \frac{1}{D} + \epsilon\,\frac{2\mu(D-1)}{D}\left(N_W - 1 + \frac{2g}{f-g}\right) + O(\epsilon^2)\,. \tag{S41}$$

In particular, the coefficient of the first-order term in ϵ becomes very small if $\mu \ll 1/(2N_W)$, meaning that for such small values of μ, we expect a strong suppression of selection, with a fixation probability that becomes independent of ϵ and flat (for very small mutational effects ϵ).

Expansion for relatively small mutational effects. Next, consider the regime where $\epsilon \ll 1$ and $N_W|\epsilon| \gg 1$ but $N_W\epsilon^2 \ll 1$. Then, if $\epsilon > 0$, Eq. S37 yields

$$\Phi_1^{\text{star}} = 1 - e^{-N_W\epsilon}\frac{D+\mu^2-1}{\mu D}\left[1 + O(\epsilon) + O(N_W\epsilon^2)\right]\,, \tag{S42}$$

which gives, employing Eq. S19,

$$\frac{\Phi_1^{\text{star}}}{\Phi_1^{\text{clique}}} = 1 + e^{-N_W\epsilon}(\mu-1)\frac{D-\mu-1}{\mu D}\left[1 + O(\epsilon) + O(N_W\epsilon^2)\right]\,. \tag{S43}$$

Thus, in this case, assuming $D > 2$, we have $\Phi_1^{\text{star}} < \Phi_1^{\text{clique}}$ if $\mu < 1$ or $\mu > D-1$, whereas $\Phi_1^{\text{star}} > \Phi_1^{\text{clique}}$ if $1 < \mu < D-1$. Now if $\epsilon < 0$, Eq. S37 yields

$$\Phi_1^{\text{star}} = \frac{1+\mu^2(D-1)}{D\,\mu^{D-1}}e^{N_W(D-1)\epsilon}\left[1 + O(\epsilon) + O(N_W\epsilon^2)\right]\,, \tag{S44}$$

which gives, employing Eq. S20,

$$\frac{\Phi_1^{\text{star}}}{\Phi_1^{\text{clique}}} = \frac{1+\mu^2(D-1)}{D\,\mu^{D-1}}\left[1 + O(\epsilon) + O(N_W\epsilon^2)\right]\,. \tag{S45}$$

Then, assuming $D > 3$, we have $\Phi_1^{\text{star}} > \Phi_1^{\text{clique}}$ if $\mu < 1$ while $\Phi_1^{\text{star}} < \Phi_1^{\text{clique}}$ if $\mu > 1$.

Combining results for $\epsilon > 0$ and $\epsilon < 0$ in this regime, as well as results obtained for very small mutational effects above, we find that the star is a suppressor of selection compared to the clique for $\mu < 1$, an amplifier of selection for $1 < \mu < D-1$, and a transient amplifier of selection for $\mu > D-1$. Indeed, in the latter case, one switches from amplification to suppression as ϵ is increased. Specifically, there is amplification for $\epsilon < 0$ satisfying $\epsilon \ll 1$ and $N_W|\epsilon| \gg 1$ but $N_W\epsilon^2 \ll 1$, and whatever the sign of ϵ in the regime where $\epsilon \ll 1$ and $N_W|\epsilon| \ll 1$, but there is suppression for $\epsilon > 0$ satisfying $\epsilon \ll 1$ and $N_W|\epsilon| \gg 1$ but $N_W\epsilon^2 \ll 1$.

Interestingly, in the regime of very small mutational effects where $\epsilon \ll 1$ and $N_W|\epsilon| \ll 1$, we showed that the strongest amplification is obtained in the limit $\mu \gg 1$, but now we find that in this case, amplification is only transient. Our expansions show that universal amplification can exist only if $1 < \mu \leq D-1$. In this case, for $\epsilon \ll 1$ and $N_W|\epsilon| \ll 1$, the strongest amplification is expected for $\mu = D-1$ (because F increases with μ, see Eq. S40), and we then have $F(D-1) = (D-2)^3/\left\{D\left[D\,(D-2)+2\right]\right\}$ so that Eq. S39 then yields

$$\frac{\Phi_1^{\text{star}}}{\Phi_1^{\text{clique}}} = 1 + \frac{\epsilon}{2}\left(N_W - 1 + \frac{2g}{f-g}\right)\frac{(D-1)(D-2)^3}{D\left[D\,(D-2)+2\right]} + O(\epsilon^2)\,. \tag{S46}$$

If $N_W \gg 1$ and $D \gg 1$, this gives a prefactor of the first order term in ϵ of order $N_W D/2$, which can yield a large amplification, but recall that this is restricted to $N_W|\epsilon| \ll 1$.

Expansion for extremely asymmetric migrations. So far we have considered expansions in selection strengths, and then in some regimes, analyzed extremely asymmetric migrations. However, the order of limits matters and our previous discussions are limited to specific regimes in terms of selection strength. If $\mu \to 0$, Eq. S37 yields

$$\Phi_1^{\text{star}} = \frac{1}{D} + O(\mu)\,, \tag{S47}$$

which demonstrates that for small m the star is a very strong suppressor of selection, with all mutations becoming effectively neutral (once they have fixed in a deme). Note that this is consistent with our result for very small mutational effects, see Eq. S41 and the discussion just below.

If $\mu \to \infty$, and in particular assuming $\mu \gg D$, Eq. S37 yields

$$\Phi_1^{\text{star}} = \frac{D-1}{D}\frac{1-\gamma^2}{1-\gamma^{2(D-1)}} + O(\mu^{-1})\,, \tag{S48}$$

and for $\gamma = N_W\rho_W/(N_M\rho_M) \to 0$, which occurs when $f_M \gg f_W$, we have $\Phi_1^{\text{star}} \to (D-1)/D$, which confirms that amplification can only be transient in this case, since for the clique, we have $\Phi_1^{\text{star}} \to 1$ in this limit. The simple expression $\Phi_1^{\text{star}} \to (D-1)/D$ is due to the fact that in the $\mu \to \infty$, mutants in the center cannot fix even if they are very fit, while those in the leaves fix easily. If in addition $D \gg 1$ (and thus $\mu \gg D \gg 1$), then

$$\Phi_1^{\text{star}} \approx \frac{1-\gamma^2}{1-\gamma^{2(D-1)}} + O(\mu^{-1})\,, \tag{S49}$$

which is formally reminiscent of the fixation probability for the star in the model of Ref. [3] with Birth-death dynamics in the limit $D \to \infty$ (see also Ref. [21]), where γ replaces the ratio of fitnesses (as is the case in Eq. 1 for the clique, which is formally reminiscent of the fixation probability for the well-mixed population). Thus, if $\mu \to \infty$ such that $\mu \gg D \gg 1$, the star can become a universal amplifier of selection with respect to the clique, and has a fixation probability identical to that of the clique but with γ replaced by γ^2, which demonstrates amplification, in the same way as in the model of Ref. [3]. However, this is restricted to the particular regime $\mu \to \infty$ such that $\mu \gg D \gg 1$.

In the Birth-death model [3], the star satisfies $m_O = 1/(D-1)$ and $m_I = 1$, so that $\mu = D-1$ (see section 3 for a more general mapping between our model and that of Ref. [3]). Let us thus consider the specific case where $\mu = D-1$. If $\mu \to \infty$ (which implies $D \to \infty$), Eq. S37 yields

$$\Phi_1^{\text{star}} = \frac{1-\gamma^2}{1-\gamma^{2(D-1)}e^{(1-\gamma^2)/\gamma}} + O(\mu^{-1})\,, \tag{S50}$$

which has the exact same form as the rigorous asymptotic expression [22] for $D \to \infty$ of the fixation probability in a star in the Birth-death model of Ref. [3]. This is consistent with the fact that Eqs. S34, S36 and S37 are exactly equivalent to the formula given in Ref. [21] with $\gamma \to f_W/f_M$ and $\mu \to D-1$ (see above). Note that the rigorous asymptotic expression from Ref. [22] is slightly different from the better known expression that has the same form as Eq. S49, which holds for $\mu \gg D \gg 1$ in our model.

Additional results for the star. In Fig. S1, we show results for the fixation probability in the star graph that complement those shown in Fig. 3.

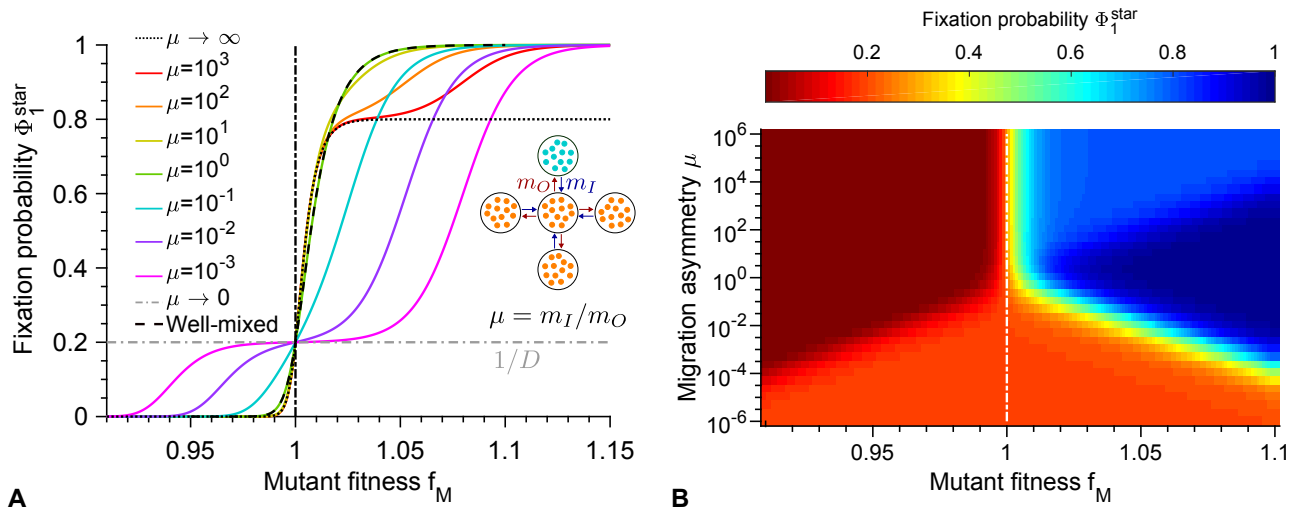

Fig S1. Fixation probability for the star. A: Fixation probability Φ_1^{star} of a mutant in a star graph versus mutant fitness f_M, starting with one fully mutant deme chosen uniformly at random, with different migration rate asymmetries $\mu = m_I/m_O$, complementing those shown in Fig. 3A. Data for the well-mixed population is shown as reference, with same total population size and initial number of mutants. Curves represent analytical predictions in Eq. S37. **B:** Heatmap of the same fixation probability Φ_1^{star} shown versus mutant fitness f_M and migration rate asymmetry $\mu = m_I/m_O$. Parameter values in both panels: $D = 5$, $K = 100$, $f_W = 1$, $g_W = g_M = 0.1$. Vertical dash-dotted lines represent the neutral case $f_W = f_M$.

3 Comparison with the model of Ref. [3]

In Ref. [3], a model where each of the N nodes of a graph is occupied by a single individual was introduced. Migration probabilities w_{ij} from node i to node j are defined along each edge ij of the graph. At each elementary step, an individual (say the one on node i) is selected for division, with probability proportional to fitness f_i, and its offspring migrates to a node j with probability w_{ij}, where it replaces the individual that was on that node. This dynamics, which became known as the Birth-death dynamics [9–11], thus allows to always maintain exactly one individual on each node. An important constraint stemming from the definition of the model is

$$\sum_{j=1}^{N} w_{ij} = 1\,, \tag{S51}$$

because the offspring of individual i has to migrate somewhere. In other words, the matrix of migration probabilities is right-stochastic. Note that self-loops where the offspring stays on the same node (corresponding to $w_{ii} > 0$) were not considered in the initial description of the model but can be added (see e.g. [16]). The probability $P_{i\to j}$ that, at a given elementary step, the offspring from node i replaces the individual in node j is given by

$$P_{i\to j} = \frac{f_i}{\sum_{k=1}^{N} f_k} w_{ij}\,, \tag{S52}$$

i.e. the probability that the individual on node i is selected for division, multiplied by the probability that its offspring migrates to node j. Note that, since exactly one replacement occurs per elementary step, $\sum_{i,j} P_{i\to j} = 1$, and that Eq. S52 satisfies this normalization constraint because Eq. S51 holds. Using Eq. S51, we can rewrite Eq. S52 as

$$P_{i\to j} = \frac{f_i w_{ij}}{\sum_{k,\,l} f_k w_{kl}}\,, \tag{S53}$$

which will be convenient for our comparison.

In our coarse-grained model, upon each migration event, the individual that migrated from deme i to deme j (with migration rate m_{ij} per individual) may fix with probability ρ_i. In particular, the probability P_i^{mut} that a specific deme i becomes mutant upon one given migration event while it was wild-type before reads

$$P_i^{\text{mut}} = \frac{\sum_{kM} N_k m_{ki}}{\sum_{k,\,j} N_k m_{kj}} \rho_i = \frac{N_M \sum_{kM} m_{ki}}{N_M \sum_{kM,\,j} m_{kj} + N_W \sum_{kW,\,j} m_{kj}} \rho_M\,, \tag{S54}$$

where $\sum_{kM}$ denotes a sum over mutant (M) demes indexed by k. In the last term we discriminated over mutant and wild-type demes and employed the fact that all demes have the same carrying capacity K, resulting in steady-state sizes N_M for mutant demes and N_W for wild-type demes, and denoted by ρ_M the fixation probability of a mutant in a wild-type deme, following our usual convention. Here, we have considered a probability upon a migration event, but migration events change the makeup of the population only if fixation ensues. To compare to the model of Ref. [3], let us instead focus only on the migration events that result into fixation. The probability $\mathcal{P}_{i\to j}$ that, upon such a successful migration event, an individual coming from deme i fixes in deme j reads

$$\mathcal{P}_{i\to j} = \frac{N_i m_{ij} \rho_i}{\sum_{k,\,l} N_k m_{kl} \rho_k} \,. \tag{S55}$$

Note that it satisfies $\sum_{i,\,j} \mathcal{P}_{i\to j} = 1$, as a fixation occurs at each successful migration event.

Eqs. S53 and S55 have the same form, with $N_i\rho_i$ in our model playing the part of f_i in the model of Ref. [3]. An important difference is that in our model, the m_{ij} (which are migration rates, not migration probabilities) do not need to satisfy the constraint in Eq. S51 and are independent. Our model is thus less constrained than that of Ref. [3]. Note that an alternative dynamics removing this constraint was discussed in Ref. [3], but then very rarely considered in the literature [11]. Note also that the fixation probability ρ_i involves the fitness of i and that of the type that is replaced (say j), but because we always work with just two types, this dependence can be ignored without losing generality.

For the clique and for the cycle, we have found that the fixation probability, given by Eq. S13, has the same form as that for the well-mixed population, but with $\gamma = N_W\rho_W/(N_M\rho_M)$ playing the part of f_W/f_M. This is perfectly consistent with the mapping described here, with $N_i\rho_i$ in our model playing the part of f_i. Note that the constraint on migration rates does not come into play here since Eq. S13 is independent of migration rates.

For the star, we already noted that the fixation probabilities given in Eqs. S34, S36 and S37 are exactly equivalent to the formula given in Ref. [21] if the following substitutions are made: $\gamma = N_W\rho_W/(N_M\rho_M) \to f_W/f_M$ and $\mu = m_I/m_O \to D-1$ (bearing in mind that in the notations of Ref. [21], $D-1$ is called n and f_W/f_M is called $1/r$). Again, this is perfectly consistent with the mapping described here, with $N_i\rho_i$ in our model playing the part of f_i. In addition, we have to impose a specific value of μ, namely $\mu = D-1$, in order to get back the result of Ref. [21]. This is because, for a star graph with no self-loops, only two different migration rates can exist, m_O from center to leaf and m_I from leaf to center, given the symmetries of this graph. Imposing that $\sum_j m_{ij}$ is independent on i, i.e. that all nodes have the same total emigration rate, which is a weaker form of the constraint in Eq. S51 (because no normalization is required on migration rates), then yields $\mu = D-1$. So the extra constraint in the mapping between the two models for the star stems from the requirement that Eq. S51 be satisfied in the model of Ref. [3]. This also means that for $\mu = D-1$, our results are formally the same as in Ref. [21] and in the model of Ref. [3] and that we then find the exact same amplification properties for the star. But this exact correspondence is restricted to a very particular value of μ.

4 Generalized circulation theorem

Here, we extend the circulation theorem from Ref. [3] to our model. Consider a metapopulation on a graph G with a set of nodes $\boldsymbol{V}$ where all D demes have the same carrying capacity. A graph with migration rates per individual m_{ij} from node i to node j is a circulation if and only if for all i,

$$\sum_{j\in\boldsymbol{V}} m_{ij} = \sum_{j\in\boldsymbol{V}} m_{ji} \,, \tag{S56}$$

which means that the total rate of migrations leaving i is equal to the total rate of migrations arriving in i. We will show that the fixation probability starting from P fully mutant demes is the same as for the clique, i.e. is given by Eq. S13, if and only if the graph G is a circulation. Let us denote by $\boldsymbol{P}$ the ensemble of fully mutant demes and by P its cardinal.

Following the proof of the circulation theorem given in Ref. [3], we will demonstrate that the following are equivalent:
(1) G is a circulation.
(2) P performs a random walk with forward bias γ^{-1}, with $\gamma = N_W\rho_W/(N_M\rho_M)$, and absorbing states $\{0, D\}$.
(3) The fixation probability starting from P fully mutant demes is the same as for the clique, i.e. is given by Eq. S13.
(4) The probability that, starting from any P fully mutant demes, a mutant such that $N_W\rho_W/(N_M\rho_M) = \gamma$

eventually fixes in P' mutant demes is given by

$$\Phi(\gamma, G, P, P') = \frac{1-\gamma^P}{1-\gamma^{P'}} \,. \tag{S57}$$

First we show that (1) $\Rightarrow$ (2), in a similar way as in Ref. [3]. For this, let $\delta_+(\boldsymbol{P})$ (resp. $\delta_-(\boldsymbol{P})$) be the probability that the number of mutant demes increases by one (resp. decreases by one). We have

$$\frac{\delta_-(\boldsymbol{P})}{\delta_+(\boldsymbol{P})} = \frac{\sum_{i\in\boldsymbol{V}\setminus\boldsymbol{P},\, j\in\boldsymbol{P}} N_W m_{ij}\rho_W}{\sum_{i\in\boldsymbol{P},\, j\in\boldsymbol{V}\setminus\boldsymbol{P}} N_M m_{ij}\rho_M} = \gamma\, \frac{\sum_{i\in\boldsymbol{V}\setminus\boldsymbol{P},\, j\in\boldsymbol{P}} m_{ij}}{\sum_{i\in\boldsymbol{P},\, j\in\boldsymbol{V}\setminus\boldsymbol{P}} m_{ij}} = \gamma\, \frac{\sum_{i\in\boldsymbol{P},\, j\in\boldsymbol{V}\setminus\boldsymbol{P}} m_{ji}}{\sum_{i\in\boldsymbol{P},\, j\in\boldsymbol{V}\setminus\boldsymbol{P}} m_{ij}} \tag{S58}$$

Since G is a circulation, Eq. S56 holds, and summing it over all $i \in \boldsymbol{P}$ yields

$$\sum_{i\in\boldsymbol{P}, j\in\boldsymbol{V}} m_{ij} = \sum_{i\in\boldsymbol{P}, j\in\boldsymbol{V}} m_{ji} \tag{S59}$$

which can be rewritten as

$$\sum_{i\in\boldsymbol{P}, j\in\boldsymbol{P}} m_{ij} + \sum_{i\in\boldsymbol{P}, j\in\boldsymbol{V}\setminus\boldsymbol{P}} m_{ij} = \sum_{i\in\boldsymbol{P}, j\in\boldsymbol{P}} m_{ji} + \sum_{i\in\boldsymbol{P}, j\in\boldsymbol{V}\setminus\boldsymbol{P}} m_{ji} \tag{S60}$$

and thus

$$\sum_{i\in\boldsymbol{P}, j\in\boldsymbol{V}\setminus\boldsymbol{P}} m_{ij} = \sum_{i\in\boldsymbol{P}, j\in\boldsymbol{V}\setminus\boldsymbol{P}} m_{ji} \tag{S61}$$

so that Eq. S58 becomes

$$\frac{\delta_-(\boldsymbol{P})}{\delta_+(\boldsymbol{P})} = \gamma \tag{S62}$$

and thus P performs a random walk with forward bias γ^{-1}.

(2) $\Rightarrow$ (3) can be proved as for the clique (see section 2.1 and Ref. [18]).

(3) $\Rightarrow$ (4) can be proved using conditional probabilities exactly as in Ref. [3].

(4) $\Rightarrow$ (1) can also be proved similarly as in Ref. [3]. Specifically, using Eq. S57 for $P = 1$ and $P' = 2$ gives

$$\Phi(\gamma, G, 1, 2) = \frac{1}{1+\gamma} \,, \tag{S63}$$

but denoting by v the initially mutant deme, we can also write the probability that 2 demes become mutant after any number k of migration events as

$$\Phi(\gamma, G, 1, 2) = \sum_{k=0}^{\infty} \left[1 - \delta_-(v) - \delta_+(v)\right]^k \delta_+(v) = \frac{\delta_+(v)}{\delta_+(v) + \delta_-(v)} \,, \tag{S64}$$

and comparing Eqs. S63 and S64 shows that for any initially mutant deme v,

$$\frac{\delta_-(v)}{\delta_+(v)} = \gamma \,. \tag{S65}$$

But Eq. S58 yields

$$\frac{\delta_-(v)}{\delta_+(v)} = \gamma\, \frac{\sum_{j\in\boldsymbol{V}\setminus v} m_{ji}}{\sum_{j\in\boldsymbol{V}\setminus v} m_{ij}} \,, \tag{S66}$$

and therefore, for all v,

$$\sum_{j\in\boldsymbol{V}\setminus v} m_{ji} = \sum_{j\in\boldsymbol{V}\setminus v} m_{ij} \,, \tag{S67}$$

which entails

$$\sum_{j\in\boldsymbol{V}} m_{ji} = \sum_{j\in\boldsymbol{V}} m_{ij} \,, \tag{S68}$$

and thus G is a circulation (see Eq. S56).

5 Comparison with the model of Ref. [13]

In Ref. [13], a model generalizing that of Ref. [3] to the case where each node of the graph is occupied by a deme with a fixed number of individuals was introduced. In the models of Refs. [3] and [13], each elementary event is composed of a death event in one deme and a birth event in another one, thus allowing to maintain constant the population of each deme. Furthermore, the order employed to choose the individual that dies and the one that divides matters for final results, yielding Birth-death and death-Birth models, as in the model introduced in Ref. [3] (see Refs. [9–11]). Conversely, in our model, migration, death and birth events are all independent. This is made possible by allowing the population size of each deme to vary. Here, we present the model of Ref. [13] and compare it to our model.

Let us consider wild-type fitness as reference and set it to 1, and let us denote mutant fitness by $1+s$. Let us denote the total number of individuals in deme i by N_i, and the number of mutant individuals in deme i by n_i. Migration probabilities w_{ij} from deme i to deme j are defined along each edge ij of the graph. We will denote by $T_i^+(\boldsymbol{n})$ the transition probability from n_i to n_i+1 and by $T_i^-(\boldsymbol{n})$ the transition probability from n_i to n_i-1, which both depend on the complete state of the system $\boldsymbol{n}=(n_1,n_2,\ldots,n_M)$.

Birth-death dynamics. In Birth-death dynamics (also known as "invasion process" [13]), the w_{ki} satisfy the normalization constraint

$$\sum_{i=1}^{D} w_{ki} = 1. \tag{S69}$$

In this dynamics, an individual is chosen for reproduction among all the individuals of the population according to its fitness. Assuming that it belongs to island k, its offspring migrates to island i with probability w_{ki}, where it replaces an individual chosen uniformly at random among the N_i individuals there. The transition probability $T_i^+(\mathbf{n})$ is given by

$$T_i^+(\boldsymbol{n}) = \underbrace{\frac{N_i-n_i}{N_i}}_{(2)} \sum_{k=1}^{D} \underbrace{w_{ki}\,\frac{n_k(1+s)}{\sum_j N_j + sn_j}}_{(1)} \tag{S70}$$

where (1) is the probability for a mutant to reproduce on island k and to migrate to i, which is then summed over all the islands k, and (2) is the probability that, given that a death event occurs on island i (because an individual in i is being replaced), a wildtype individual dies. Analogously:

$$T_i^-(\boldsymbol{n}) = \frac{n_i}{N_i} \sum_{k=1}^{D} w_{ki}\,\frac{N_k-n_k}{\sum_j N_j + sn_j}. \tag{S71}$$

Death-birth dynamics. In death-Birth dynamics (also known as "voter model" [13]), we assume that $\sum_k w_{ki}=1$. In this dynamics, an individual is chosen uniformly at random in the entire population to die. Assuming that death occurred in island i, one may consider that a migration event then occurs from island k to i with probability w_{ki}. But one may also assume that migration occurs from k to i with a probability proportional to the product of w_{ki} and the total fitness N_k+sn_k of island k. The first choice considers fitness to be relevant only within each island, while the second one takes into account fitness across the islands. We will consider the second one because it allows to recover the usual death-Birth model [9–11] when $N_i=1\,\forall i\in\{1,\ldots,D\}$. Finally, the reproducing individual on island i is chosen according to its fitness within the island. The transition probability $T_i^+(\boldsymbol{n})$ reads

$$T_i^+(\boldsymbol{n}) = \underbrace{\frac{N_i-n_i}{\sum_j N_j}}_{(1)} \sum_{k=1}^{D} \underbrace{\frac{w_{ki}(N_k+sn_k)}{\sum_j w_{ji}(N_j+sn_j)}}_{(2)} \underbrace{\frac{n_k(1+s)}{N_k+sn_k}}_{(3)} = \frac{N_i-n_i}{\sum_j N_j}\,\frac{\sum_k w_{ki}n_k(1+s)}{\sum_j w_{ji}(N_j+sn_j)} \tag{S72}$$

where (1) is the probability for a wildtype individual to die on island i, while (2) is the probability that, given that a death event occurs on island i, a migration event occurs from island k to i, which takes into account the total fitness of island k. Finally, (3) is the probability that, given that a reproduction event happens in island k, it is a mutant who reproduces. Similarly,

$$T_i^-(\boldsymbol{n}) = \frac{n_i}{\sum_j N_j}\,\frac{\sum_k w_{ki}(N_k-n_k)}{\sum_j w_{ji}(N_j+sn_j)}\,. \tag{S73}$$

Clique. Consider a clique made of D demes of size N (all of identical and composition-independent size), such that $w_{ij} = w$ for all $i \neq j$ and $w_{ii} = w'$ for all i. If migrations between different demes are rare enough, one can coarse-grain the process and consider that each deme is either fully mutant or fully wild-type, and the state of the clique can then be fully described by the number α of mutant demes, which changes when migrations followed by fixation occur. In the Birth-death model, starting from Eq. S71 and summing over mutant demes, we obtain

$$T_\alpha^+ = \frac{\alpha(D-\alpha)}{D+s\alpha} w(1+s)\rho_M \,, \tag{S74}$$

and similarly

$$T_\alpha^- = \frac{\alpha(D-\alpha)}{D+s\alpha} w\rho_W \,, \tag{S75}$$

which entails that

$$\gamma = \frac{T_\alpha^-}{T_\alpha^+} = \frac{(1+s)\rho_M}{\rho_W} = \frac{\rho_M f_M}{\rho_W f_W} \,, \tag{S76}$$

and thus the probability that the mutant fixes in the whole population starting from i mutant demes is given by Eq. S13 but with γ expressed in Eq. S76. The same result is obtained in the death-Birth case.

Star. We consider the star graph with self-loops (i.e. allowing replacement within a given deme, corresponding to migration from this deme to itself, $w_{ii} > 0$). Indeed, the rare migration regime that we study in our model means in the framework of the model of Ref. [13] that replacement is much more frequent within a deme than across two demes, thus requiring very strong self-loops, i.e. large w_{ii} values. While the star with self-loops was introduced in Ref. [16] with one individual per node of the graph, in the spirit of Ref. [3], here we treat it in the model of Ref. [13], where each node contains a deme with fixed size N. Following Ref. [16], we introduce two parameters x and y ($0 < x, y \leq 1$) such that $1-y$ is the weight of the self-loop of the center and $1-x$ is the weight of the self-loops on each leaf. The other weights are chosen in order to respect the symmetry of the star and for W to be right stochastic in the Birth-death case and left stochastic in the death-Birth case. Hence, in the Birth-death model, the matrix of migration probabilities reads:

$$W = \begin{pmatrix} 1-y & y/(D-1) & y/(D-1) & \cdots & y/(D-1) & y/(D-1) \\ x & 1-x & 0 & \cdots & 0 & 0 \\ x & 0 & 1-x & \cdots & 0 & 0 \\ \vdots & \vdots & \vdots & \ddots & \vdots & \vdots \\ x & 0 & 0 & \cdots & 1-x & 0 \\ x & 0 & 0 & \cdots & 0 & 1-x \end{pmatrix} , \tag{S77}$$

where nodes are numbered so that the first one is the center of the star and others are leaves. The case $x = y = 1$ corresponds to the star without self-loops introduced in Ref. [3].

In order to compare our model to the model of Ref. [13] in the case of the star, we choose their respective parameters so that in each deme, both models have the same value for the ratio of the migration rate T_{mig} leaving the deme to the reproduction rate T_{rep} in the same deme. In our model, the reproduction rate per individual is given by $T_{rep} = f_W(1 - N_W/K)$ for each deme, whatever its type (leaf or center) – in the wild-type case. Still in our model, the migration rate leaving the center (to any leaf) is $m_O(D-1)$ per individual, and that leaving a leaf (to the center, which is the only possibility) is m_I per individual. In the framework of the Birth-death model of Ref. [13], the total reproduction probability per individual in a deme (irrespective of where the offspring from this deme migrates) is equal to $\sum_j w_{ij} = 1$, for both the center and for a leaf, while the total migration probability per individual leaving the center is $\sum_{j\neq 1} w_{1j} = y$ and the one leaving a leaf is $\sum_{j\neq i} w_{ij} = x$ with $i > 1$ (see Eq. S77). Thus, to match our model with the Birth-death model of Ref. [13], we have the following two constraints:

$$y = \frac{m_O(D-1)}{f_W(1-N_W/K)} \,, \tag{S78}$$

and

$$x = \frac{m_I}{f_W(1-N_W/K)} \,. \tag{S79}$$

Fig. S2A shows that once this matching is done, a good agreement is obtained between simulation results for the two models, which yield similar mutant fixation probabilities across various migration asymmetries μ. Figs. S2B and C show small relative and absolute differences, respectively, between the two models. Note that the relative error is high when the probability of fixation of a mutant deme is close to zero, which is the case for deleterious mutations, but then the absolute error is small, which confirms that these models are consistent.

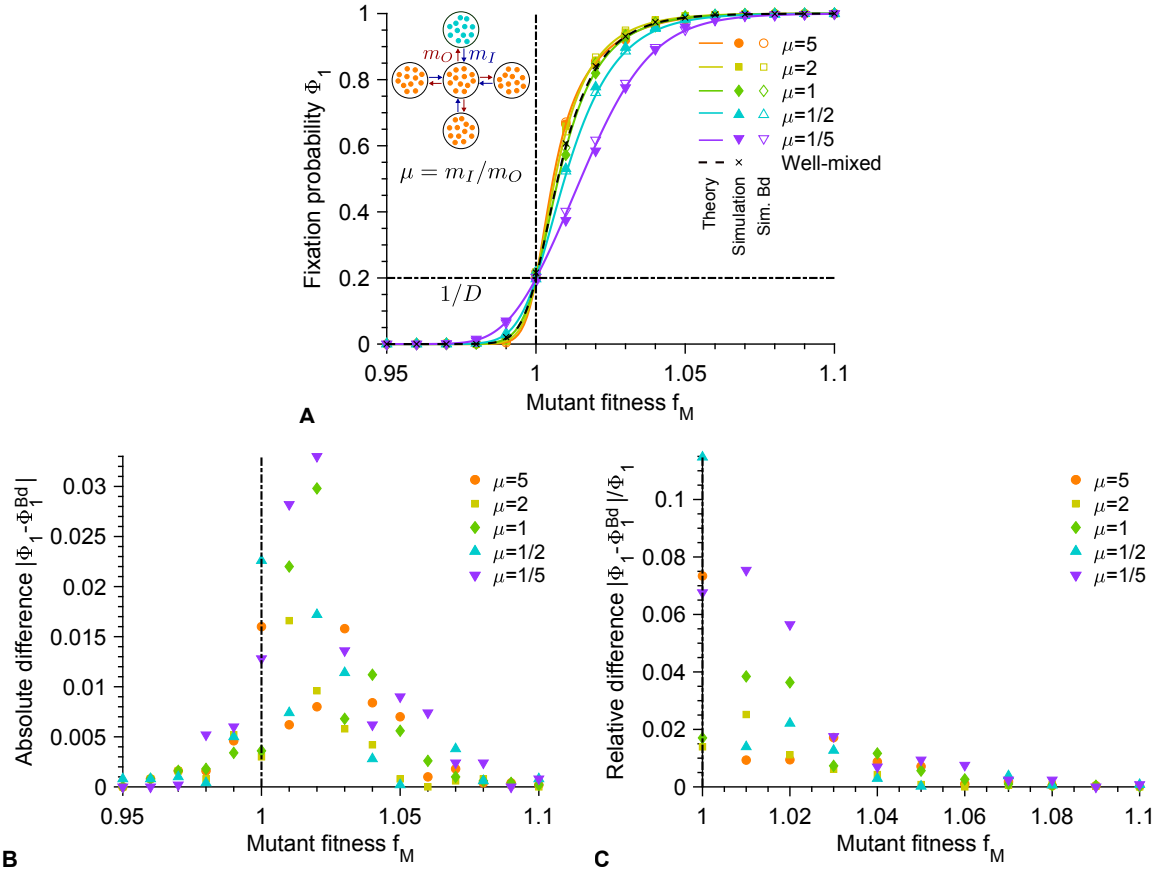

Fig S2. Comparison between the Birth-death model inspired by Refs. [13] and [16] and our model. **A:** Fixation probability Φ_1 of a mutant in a star graph versus mutant fitness f_M, starting with one fully mutant deme chosen uniformly at random, with different migration rate asymmetries $\mu = m_I/m_O$ in our model and in the matching Birth-death (Bd) model, which satisfies Eqs. S78 and S79. Markers are obtained from 2×10^3 stochastic simulation realizations in our model, and in the Bd model of Ref. [13]. Curves represent analytical predictions for our model in Eqs. S34, S36 and S37. **B:** Absolute differences between simulation results obtained with the two models (see panel **A**), as a function of the mutant fitness f_M. **C:** Relative differences between simulation results obtained with the two models (see panel **A**), as a function of the mutant fitness f_M. Parameter values for our model: $D = 5$, $K = 100$, $f_W = 1$, $g_W = g_M = 0.1$, and from top to bottom in the legend of panel **A**, $(m_I, m_O) \times 10^6 = (5, 1)$; $(2, 1)$; $(1, 1)$; $(1, 2)$; $(1, 5)$ in simulations, as in Fig. 3. Parameter values for the matching Birth-death model: $D = 5$, $N = N_W = 90$, $f_W = 1$, and values of x and y satisfying Eqs. S78 and S79 for each pair of values of m_I and m_O from our model. Vertical dash-dotted lines indicate the neutral case $f_W = f_M$.

The Birth-death model of Ref. [13] has the same total reproduction rate in each deme. Once the matching in Eqs. S78 and S79 is done, it also features the same migration-to-reproduction ratio as in our model. Note however that the death rate is not uniform across demes in this model: in the center it is $\sum_i w_{i1} = 1 - y + (D-1)x$, and in a leaf it is $\sum_i w_{ij} = 1 - x + y/(D-1)$ with $j > 1$. This stands in contrast with our model, and to resolve this discrepancy, we would need to impose that $y = (D-1)x$. In that case, the matrix of migration probabilities in Eq. S77 becomes doubly stochastic and the star becomes a circulation, and thus it has the same fixation probability as the clique in the model of Ref. [13] (see above). Consistently, Eqs. S78 and S79 then entail $\mu = 1$. This shows that the matching between models is not perfect for other values of μ, because the model of Ref. [13] is more constrained than our model, as it imposes constant deme size.

In the death-Birth model, the matrix of migration probabilities is the transpose of that given in Eq. S77. Hence, the total reproduction rates for a leaf and the center are $\sum_i w_{ij} = y/(D-1) + 1 - x$ with $j > 1$ and $\sum_i w_{i1} = 1 - y + (D-1)x$, respectively, while the total migration rates per individual from a leaf and from the center are $y/(D-1)$ and $(D-1)x$, respectively. Thus, to match our model with the death-Birth model, we have the

following two constraints:

$$x f_W \left(1 - \frac{N_W}{K}\right) = m_O(1 - y + (D-1)x)\,, \tag{S80}$$

and

$$\frac{y}{D-1} f_W \left(1 - \frac{N_W}{K}\right) = m_I \left(\frac{y}{D-1} + 1 - x\right)\,. \tag{S81}$$

In this case too, Fig. S3 shows that once this matching is done, a good agreement is obtained between simulation results for the two models.

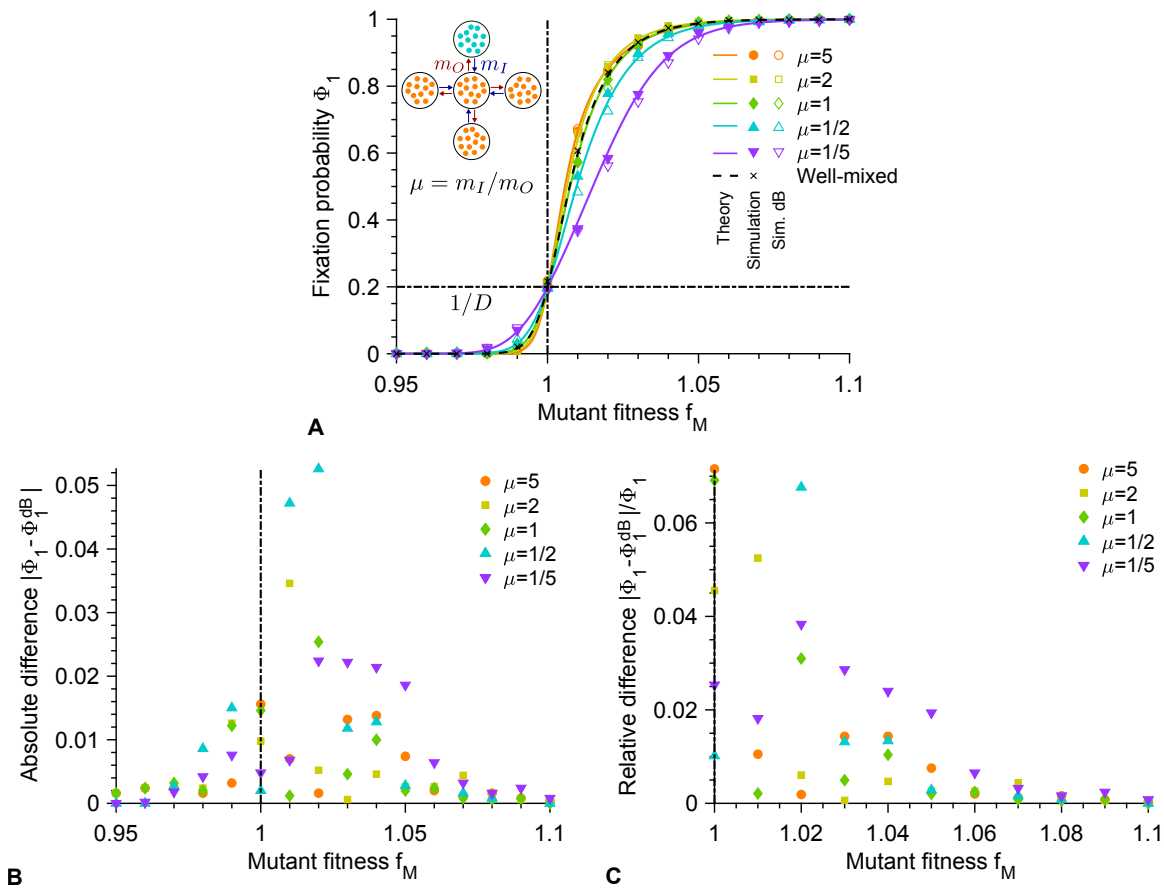

Fig S3. Comparison between the death-Birth model inspired by Refs. [13] and [16] and our model. **A:** Fixation probability Φ_1 of a mutant in a star graph versus mutant fitness f_M, starting with one fully mutant deme chosen uniformly at random, with different migration rate asymmetries $\mu = m_I/m_O$ in our model and in the matching death-Birth (dB) model, which satisfies Eqs. S80 and S81. Markers are obtained from 2×10^3 stochastic simulation realizations in our model, and in the dB model of Ref. [13]. Curves represent analytical predictions for our model in Eqs. S34, S36 and S37. **B:** Absolute differences between simulation results obtained with the two models (see panel **A**), as a function of the mutant fitness f_M. **C:** Relative differences between simulation results obtained with the two models (see panel **A**), as a function of the mutant fitness f_M. Parameter values for our model: $D = 5$, $K = 100$, $f_W = 1$, $g_W = g_M = 0.1$, and from top to bottom in the legend of panel **A**, $(m_I, m_O) \times 10^6 = (5, 1)$; $(2, 1)$; $(1, 1)$; $(1, 2)$; $(1, 5)$ in simulations, as in Fig. 3. Parameter values for the matching death-Birth model: $D = 5$, $N = N_W = 90$, $f_W = 1$, and values of x and y satisfying Eqs. S80 and S81 for each pair of values of m_I and m_O from our model. Vertical dash-dotted lines indicate the neutral case $f_W = f_M$.

The death-Birth model of Ref. [13] has the same total death rate in each deme. Once the matching in Eqs. S78 and S79 is done, it also features the same migration-to-reproduction ratio as in our model. Note however that the birth rate is not uniform across demes in this model even in the absence of fitness differences (see above). Here too, to resolve this discrepancy with our model, we would need to impose that $y = (D-1)x$, with the same consequences as in the Birth-death model – note that Birth-death and death-Birth models then yield the same result. Again, this

shows that the matching between models is not perfect for other values of μ, because the model of Ref. [13] is more constrained than our model, as it imposes constant deme size.

6 A simple structure with different population sizes: the doublet

Let us consider a doublet made of two demes with different sizes linked by migration. The large deme has carrying capacity K_L and the small deme has carrying capacity K_S. The migration rate per individual from the small deme to the large one is m_S, and that from the large to the small deme by m_L. We start from exactly one fully mutant deme.

Let us first consider the case where the small deme, whose carrying capacity is denoted by K_S, is fully mutant, while the large deme, whose carrying capacity is denoted by K_L, is fully wild-type. If an M individual migrates from the small deme to the large deme and fixes, then the mutant type fixes in the whole population. The probability that this occurs upon a given migration event reads

$$T_S^+ = \frac{m_L N_M^S}{m_L N_M^S + m_S N_W^L} \rho_M^L \,, \tag{S82}$$

where $N_M^S = K_S(1 - g_M/f_M)$ (respectively $N_W^L = K_L(1 - g_W/f_W)$) is the equilibrium size of the small mutant deme (respectively of the large wild-type deme) and ρ_M^L is the fixation probability of a mutant in the large wild-type deme, given by Eq. S7 with N_W^L instead of N_W. Similarly, if a W individual migrates to the small deme and fixes, then the wild-type fixes in the whole population. The probability that this occurs upon a given migration event reads

$$T_S^- = \frac{m_S N_W^L}{m_L N_M^S + m_S N_W^L} \rho_W^S \,, \tag{S83}$$

where ρ_W^S is the fixation probability of a wild-type individual in the small mutant deme, given by Eq. S10 with N_M^S instead of N_M. Then, the fixation probability of the mutant type, starting from a small mutant deme and a large wild-type deme, reads

$$\Phi_{1,S}^{\text{doublet}} = \frac{T_S^+}{T_S^+ + T_S^-} = \frac{m_L N_M^S \rho_M^L}{m_L N_M^S \rho_M^L + m_S N_W^L \rho_W^S} = \frac{1}{1 + \mu \gamma_S} \,, \tag{S84}$$

where $\mu = m_S/m_L$ and $\gamma_S = N_W^L \rho_W^S / (N_M^S \rho_M^L)$.

Similarly, in the case where the structured population starts from a large mutant deme, while the small deme is wild-type, we get the fixation probability

$$\Phi_{1,L}^{\text{doublet}} = \frac{m_S N_M^L \rho_M^S}{m_S N_M^L \rho_M^S + m_L N_W^S \rho_W^L} = \frac{1}{1 + \gamma_L/\mu} \,, \tag{S85}$$

where $\gamma_L = N_W^S \rho_W^L / (N_M^L \rho_M^S)$.

Next, consider the case where one mutant individual starts in a deme with a probability proportional to the size of the deme, which corresponds to the realistic case of mutations happening randomly upon division. The fixation probability of such a single mutant reads:

$$\rho_M^{\text{doublet}} = \frac{K_S}{K_S + K_L} \rho_M^S \Phi_{1,S}^{\text{doublet}} + \frac{K_L}{K_S + K_L} \rho_M^L \Phi_{1,L}^{\text{doublet}} \,. \tag{S86}$$

In the rest of this work, which focuses on structured populations made of demes of identical sizes, we consider the fixation probability Φ_1 starting from one fully mutant deme, which then needs to be multiplied by ρ_M to obtain that of one mutant individual. Here, we will consider the analogous quantity

$$\Phi_1^{\text{doublet}} = \frac{\rho_M^{\text{doublet}}}{\rho_M^S} = \frac{K_S}{K_S + K_L} \Phi_{1,S}^{\text{doublet}} + \frac{K_L}{K_S + K_L} \frac{\rho_M^L}{\rho_M^S} \Phi_{1,L}^{\text{doublet}} \,. \tag{S87}$$

In the particular case where $K_L = (D-1)K_S$, so that the total carrying capacity of the subdivided population is DK_S, denoting K_S by K, considering Φ_1^{doublet} allows for a direct comparison to Φ_1 in the other structures considered here, comprising D demes of carrying capacity K.

Expansion for relatively small mutational effects. For the sake of simplicity, here we assume that $K_L = (D-1)K_S$, so that the total carrying capacity of the subdivided population is DK_S, and we further denote K_S by K. Consider the regime where $\epsilon \ll 1$ and $N_W|\epsilon| \gg 1$ but $N_W\epsilon^2 \ll 1$. Then, if $\epsilon > 0$, Eqs. S84, S85 and S87 yield

$$\Phi_1^{\text{doublet}} = 1 - (\mu+1)\frac{D-1}{D}e^{-N_W\epsilon}\left[1 + O(\epsilon) + O(N_W\epsilon^2)\right] , \tag{S88}$$

which gives, employing Eq. S19,

$$\frac{\Phi_1^{\text{doublet}}}{\Phi_1^{\text{clique}}} = 1 + \frac{1-\mu\,(D-1)}{D}e^{-N_W\epsilon}\left[1 + O(\epsilon) + O(N_W\epsilon^2)\right] . \tag{S89}$$

Thus, in this case, assuming $D > 1$, we have $\Phi_1^{\text{doublet}} > \Phi_1^{\text{clique}}$ if $\mu < 1/(D-1)$, whereas $\Phi_1^{\text{doublet}} < \Phi_1^{\text{clique}}$ if $\mu > 1/(D-1)$. Now if $\epsilon < 0$, Eqs. S84, S85 and S87 yield

$$\Phi_1^{\text{doublet}} = \frac{1+\mu^2\,(D-1)^3}{\mu D\,(D-1)}e^{N_W(D-1)\epsilon}\left[1 + O(\epsilon) + O(N_W\epsilon^2)\right] , \tag{S90}$$

which gives, employing Eq. S20,

$$\frac{\Phi_1^{\text{doublet}}}{\Phi_1^{\text{clique}}} = \frac{1+\mu^2\,(D-1)^3}{\mu D\,(D-1)}\left[1 + O(\epsilon) + O(N_W\epsilon^2)\right] . \tag{S91}$$

Then, assuming $D > 2$, studying the function $G : \mu \mapsto \left[1+\mu^2(D-1)^3\right] / \left[\mu D\,(D-1)\right]$ demonstrates that $\Phi_1^{\text{doublet}} > \Phi_1^{\text{clique}}$ if $\mu < 1/(D-1)^2$ or $\mu > 1/(D-1)$, whereas $\Phi_1^{\text{doublet}} < \Phi_1^{\text{clique}}$ if $1/(D-1)^2 < \mu < 1/(D-1)$. Therefore, in the regime where $\epsilon \ll 1$ and $N_W|\epsilon| \gg 1$ but $N_W\epsilon^2 \ll 1$, the doublet is an amplifier of selection with respect to the clique for $1/(D-1)^2 < \mu < 1/(D-1)$, and a suppressor of selection for $\mu > 1/(D-1)$. Finally, for $\mu < 1/(D-1)^2$, it behaves as a suppressor for $\epsilon < 0$ and as an amplifier for $\epsilon > 0$.

Expansion for extremely asymmetric migrations. If $\mu \to 0$, then Eqs. S84, S85 and S87 yield

$$\Phi_1^{\text{doublet}} \approx \frac{1}{D} , \tag{S92}$$

while if $\mu \to \infty$, they give

$$\Phi_1^{\text{doublet}} \approx \frac{D-1}{D}\frac{\rho_M^L}{\rho_M^S} . \tag{S93}$$

Additional results for the doublet. In Fig. S4, we show results for the fixation probability in the star graph that complement those shown in Fig. 5.

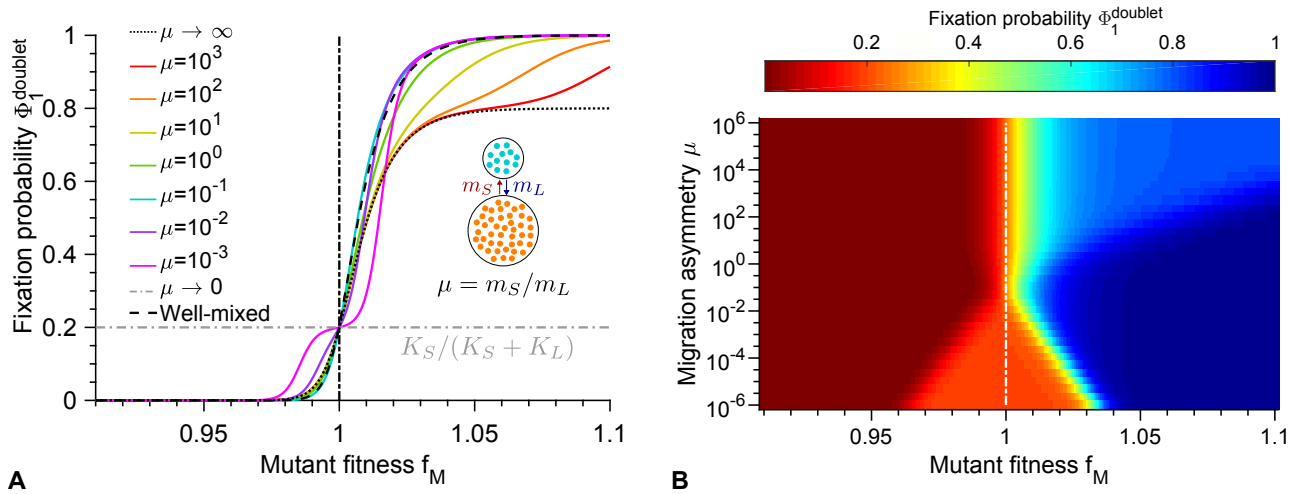

Fig S4. Fixation probability for the doublet. A: Fixation probability Φ_1^{doublet} of a mutant in a doublet versus mutant fitness f_M, starting with one fully mutant deme chosen proportionally, with different migration rate asymmetries $\mu = m_S/m_L$, complementing those shown in Fig. 5. Data for the well-mixed population is shown as reference, with same total population size and initial number of mutants. Curves represent analytical predictions in Eqs. S84, S85 and S87. **B**: Heatmap of the same fixation probability versus mutant fitness f_M and migration rate asymmetry $\mu = m_S/m_L$. Parameter values in both panels: $K_S = 100$, $K_L = 400$ (hence $K_L = (D-1)K_S$ with $K_S = K = 100$ and $D = 5$), $f_W = 1$, $g_W = g_M = 0.1$. Vertical dash-dotted lines represent the neutral case $f_W = f_M$.

7 Constant deme size approximation

In our model, we consider that the number of individuals in each deme is not fixed, but there is a carrying capacity K per deme. In a deterministic description, valid for large populations, if there is only one type of individuals, the number N of individuals at time t follows the ordinary differential equation:

$$\frac{\mathrm{d}N}{\mathrm{d}t} = \left[f\left(1 - \frac{N}{K}\right) - g \right] N \ , \tag{S94}$$

where f represents fitness, g death rate and K carrying capacity. If $f > g$, Eq. S94 yields a nonzero steady-state population size, namely $K(1 - g/f)$. In a stochastic description, a finite-size microbial population with a logistic growth rate and a constant death rate fluctuates around the deterministic steady-state average population size $K(1 - g/f)$ after a transient time depending on initial conditions and before eventually going extinct (after a very long time if it carrying capacity is not small) [43, 44]. Therefore, in our analytical studies, we often employ the steady-state population sizes of wild-type and mutant demes, denoted by N_W and N_M respectively:

$$N_W = K(1 - g_W/f_W) \ , \tag{S95}$$

and

$$N_M = K(1 - g_M/f_M) \ . \tag{S96}$$

Furthermore, for simplicity, we approximate fixation probabilities in each deme by their values computed at fixed population size within the Moran process [19, 20]. The fixation probability of a single mutant (resp. wild-type) in a wild-type (resp. mutant) deme of steady-state size N_W (resp. N_M) is then given by Eq. S7 (resp. Eq. S10). This approximation is expected to be reasonable for large enough steady-state deme sizes. This is confirmed by Fig. S5, where the constant-size approximation from Eq. S7 is compared to results from stochastic simulations of the evolutionary dynamics of a mutant in a population of W individuals with variable population size, and to a numerical resolution of the Master equation for variable population size, based on Ref. [45]. In the cases with variable population size, we use a carrying capacity K and a steady-state size $N_W = K(1 - g_W/f_W)$, as in the rest of our work.

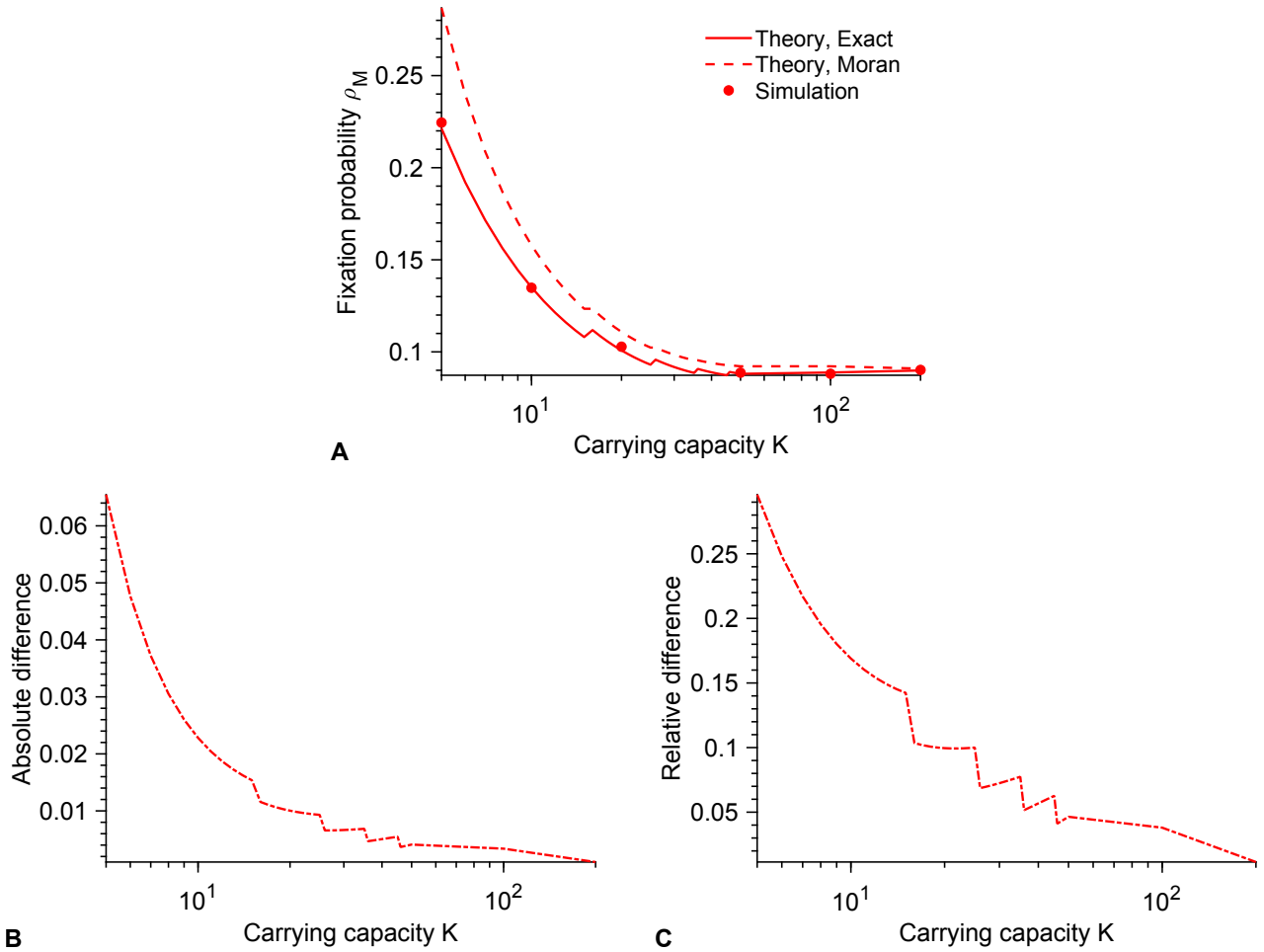

Fig S5. Constant deme size approximation. Fixation probability ρ_M of a mutant in a population of wild-type individuals with carrying capacity K and steady-state size $N_W = K(1 - g_W/f_W)$. Markers: averages over 10^4 stochastic simulations. Solid line: numerical resolution of the Master equation, see Eq. 3 in Ref. [45]. Dashed line: constant-size approximation employed in this work, in the framework of the Moran process [19, 20] (see Eq. S7). Parameter values: $f_W = 1$, $f_M = 1.1$, $g_W = g_M = 0.1$. Absolute and relative differences between the dashed and solid lines of panel **A** are shown in panels **B** and **C**. Discontinuities arise from the need to set the constant population size in the Moran to an integer value, while the steady-state size is not necessarily an integer – this is done by truncation.

8 Simulation methods

Our numerical simulations are performed using a Gillespie algorithm that is exact and does not involve any artificial discretization of time [46,47]. We focus on the regime where deme sizes N_i fluctuate weakly around their deterministic steady-state values, namely $N_i = K_i(1-g_a/f_a)$ if all microbes in deme i are of type a. Thus, we start our simulations at these sizes, and we consider K_i large enough for stochastic extinctions not to occur within the timescales studied. In most cases, we start our simulations with one fully mutant deme, while all others are fully wild-type, because this describes the second step in the fixation of a mutant (after it has fixed in a deme) in the rare migration regime. Note however that our stochastic simulations are valid beyond the rare migration regime and allow us to test the validity of this assumption and to go beyond this regime. We consider a structured population of D demes labeled $i = 1, 2, ..., D$, and denote by $N_{W,i}$ and $N_{M,i}$ the respective numbers of W and M individuals in deme i.

The elementary events that can happen are reproduction, death and migration of an individual of either type:

- $W_i \overset{k^+_{W,i}}{\rightarrow} 2W_i$: Reproduction of a wild-type microbe in deme i with rate $k^+_{W,i} = f_W[1-(N_{W,i}+N_{M,i})/K]$.
- $W_i \overset{k^-_{W,i}}{\rightarrow} \emptyset$: Death of a wild-type microbe in deme i with rate $k^-_{W,i} = g_W$.
- $M_i \overset{k^+_{M,i}}{\rightarrow} 2M_i$: Reproduction of a mutant microbe in deme i with rate $k^+_{M,i} = f_M[1-(N_{W,i}+N_{M,i})/K]$.
- $M_i \overset{k^-_{M,i}}{\rightarrow} \emptyset$: Death of a mutant microbe in deme i with rate $k^-_{M,i} = g_M$. Note that we take $g_M = g_W$ throughout.
- $W_i \overset{m_{ij}}{\rightarrow} W_j$: Migration of a wild-type microbe from deme i to deme j with rate m_{ij}.
- $M_i \overset{m_{ij}}{\rightarrow} M_j$: Migration of a mutant microbe from deme i to deme j with rate m_{ij}.

The total rate of events is given by $k_{tot} = \sum_{i=1}^{D}\left(k^+_{W,i}+k^-_{W,i}\right)N_{W,i}+\left(k^+_{M,i}+k^-_{M,i}\right)N_{M,i}+\sum_{i,j=1}^{D} m_{ij}\left(N_{W,i}+N_{M,i}\right)$.

Simulation steps are as follows:

1. Initialization: All of the D demes start from either $N_W = K(1-g_W/f_W)$ wild-type microbes or $N_M = K(1-g_M/f_M)$ mutant microbes, at time $t = 0$.
2. Monte Carlo step: Time t is incremented by Δt, sampled from an exponential distribution with mean $1/k_{tot}$. The next event to occur is chosen proportionally to its probability k/k_{tot}, where k is its rate, and is executed.
3. We go back to Step 2 unless only one type of individuals, either W or M, remains in the population, which corresponds to fixation of one type. Simulation is ended when fixation occurs.

Our simulations were coded in the C programming language.

References

1. van Marle G, Gill MJ, Kolodka D, McManus L, Grant T, Church DL. Compartmentalization of the gut viral reservoir in HIV-1 infected patients. Retrovirology. 2007;4:87.
2. Schnell G, Price RW, R S, Spudich S. Compartmentalization and clonal amplification of HIV-1 variants in the cerebrospinal fluid during primary infection. J Virol. 2010;84:2395.
3. Lieberman E, Hauert C, Nowak MA. Evolutionary dynamics on graphs. Nature. 2005;433(7023):312–316.
4. Wright S. Evolution in Mendelian populations. Genetics. 1931;16(2):97–159.
5. Kimura M, Weiss GH. The Stepping Stone Model of Population Structure and the Decrease of Genetic Correlation with Distance. Genetics. 1964;49(4):561–576.
6. Maruyama T. On the fixation probability of mutant genes in a subdivided population. Genet Res. 1970;15:221–225.
7. Maruyama T. A simple proof that certain quantities are independent of the geographical structure of population. Theor Popul Biol. 1974;5(2):148–154.
8. Barton N. The probability of fixation of a favoured allele in a subdivided population. Genet Res. 1993;62:149–157.
9. Kaveh K, Komarova NL, Kohandel M. The duality of spatial death-birth and birth-death processes and limitations of the isothermal theorem. Royal Society Open Science. 2015;2(4):140465.
10. Hindersin L, Traulsen A. Most Undirected Random Graphs Are Amplifiers of Selection for Birth-Death Dynamics, but Suppressors of Selection for Death-Birth Dynamics. PLOS Computational Biology. 2015;11(11):1–14.
11. Pattni K, Broom M, Rychtář J, Silvers LJ. Evolutionary graph theory revisited: when is an evolutionary process equivalent to the Moran process? Proceedings of the Royal Society A: Mathematical, Physical and Engineering Sciences. 2015;471(2182):20150334.
12. Campos PR, Combadão J, Dionisio F, Gordo I. Muller's ratchet in random graphs and scale-free networks. Phys Rev E Stat Nonlin Soft Matter Phys. 2006;74(4 Pt 1):042901.
13. Houchmandzadeh B, Vallade M. The fixation probability of a beneficial mutation in a geographically structured population. New Journal of Physics. 2011;13(7):073020.
14. Houchmandzadeh B, Vallade M. Exact results for fixation probability of bithermal evolutionary graphs. Biosystems. 2013;112(1):49–54.
15. Constable GW, McKane AJ. Population genetics on islands connected by an arbitrary network: an analytic approach. J Theor Biol. 2014;358:149–165.
16. Adlam B, Chatterjee K, Nowak MA. Amplifiers of selection. Proc R Soc A. 2015;471:20150114.
17. Allen B, Sample C, Jencks R, Withers J, Steinhagen P, Brizuela L, et al. Transient amplifiers of selection and reducers of fixation for death-Birth updating on graphs. PLoS Comput Biol. 2020;16(1):e1007529.
18. Traulsen A, Hauert C. 2. In: Stochastic Evolutionary Game Dynamics. John Wiley and Sons, Ltd; 2010. p. 25–61.
19. Moran PAP. Random processes in genetics. Mathematical Proceedings of the Cambridge Philosophical Society. 1958;54(1):60–71.
20. Ewens WJ. Mathematical Population Genetics. Springer-Verlag; 1979.
21. Broom B, Rychtář J. An analysis of the fixation probability of a mutant on special class of non-directed graphs. Proceedings of The Royal Society A: Mathematical, Physical and Engineering Sciences. 2008;464.
22. Chalub FACC. An asymptotic expression for the fixation probability of a mutant in star graphs. J Dynamics and Games. 2016;3(3):217–223.

23. Frean M, Baxter G. Death-birth ordering and suppression of fitness in networks. Preprint: `http://homepagesmcsvuwacnz/~marcus/manuscripts/FreanBaxterJTBpdf`. 2008;.

24. Hadjichrysanthou C, Broom M, Rychtář J. Evolutionary Games on Star Graphs Under Various Updating Rules. Dyn Games Appl. 2011;1:386.

25. Traulsen A, Sengupta AM, Nowak MA. Stochastic evolutionary dynamics on two levels. J Theor Biol. 2005;235(3):393–401.

26. Alonso D, Etienne RS, McKane AJ. The merits of neutral theory. Trends Ecol Evol. 2006;21(8):451–457.

27. Ohtsuki H, Hauert C, Lieberman E, Nowak MA. A simple rule for the evolution of cooperation on graphs and social networks. Nature. 2006;441(7092):502–505.

28. Taylor PD, Day T, Wild G. Evolution of cooperation in a finite homogeneous graph. Nature. 2007;447(7143):469–472.

29. Débarre F. Fidelity of parent-offspring transmission and the evolution of social behavior in structured populations. J Theor Biol. 2017;420:26–35.

30. Zukewich J, Kurella V, Doebeli M, Hauert C. Consolidating birth-death and death-birth processes in structured populations. PLoS One. 2013;8(1):e54639.

31. Tkadlec J, Pavlogiannis A, Chatterjee K, Nowak MA. Limits on amplifiers of natural selection under death-Birth updating. PLoS Comput Biol. 2020;16(1):e1007494.

32. Baxter GJ, Blythe RA, McKane AJ. Fixation and consensus times on a network: a unified approach. Phys Rev Lett. 2008;101(25):258701.

33. Frean M, Rainey PB, Traulsen A. The effect of population structure on the rate of evolution. Proc Biol Sci. 2013;280(1762):20130211.

34. Hauert C, Chen YT, Imhof LA. Fixation Times in Deme Structured, Finite Populations with Rare Migration. J Stat Phys. 2014;156:739–759.

35. Hindersin L, Traulsen A. Counterintuitive properties of the fixation time in network-structured populations. J R Soc Interface. 2014;11(99).

36. Lombardo P, Gambassi A, Dall'Asta L. Nonmonotonic effects of migration in subdivided populations. Phys Rev Lett. 2014;112(14):148101.

37. Allen B, Sample C, Dementieva Y, Medeiros RC, Paoletti C, Nowak MA. The molecular clock of neutral evolution can be accelerated or slowed by asymmetric spatial structure. PLoS Comput Biol. 2015;11(2):e1004108.

38. Hathcock D, Strogatz SH. Fitness dependence of the fixation-time distribution for evolutionary dynamics on graphs. Phys Rev E. 2019;100(1-1):012408.

39. Pavlogiannis A, Tkadlec J, Chatterjee K, Nowak MA. Construction of arbitrarily strong amplifiers of natural selection using evolutionary graph theory. Commun Biol. 2018;1:71.

40. Bansept F, Marrec L, Bitbol AF, Loverdo C. Antibody-mediated crosslinking of gut bacteria hinders the spread of antibiotic resistance. Evolution. 2019;73(6):1077–1088.

41. Oh KW, Ahn CH. A review of microvalves. J Micromech Microeng. 2006;16:R13.

42. Arnold FH, Volkov AA. Directed evolution of biocatalysts. Curr Opin Chem Biol. 1999;3(1):54–59.

43. Vogels M, Zoeckler R, Stasiw DM, Cerny LC. P. F. Verhulst's "notice sur la loi que la populations suit dans son accroissement" from correspondence mathematique et physique. Ghent, vol. X, 1838. Journal of Biological Physics. 1975;3(4):183–192.

44. Ovaskainen O, Meerson B. Stochastic models of population extinction. Trends Ecol Evol. 2010;25(11):643 – 652.

45. Parsons TL, Quince C. Fixation in haploid populations exhibiting density dependence I: The non-neutral case. Theor Popul Biol. 2007;72(1):121–135.

46. Gillespie DT. A general method for numerically simulating the stochastic time evolution of coupled chemical reactions. J Comput Phys. 1976;22:403–434.

47. Gillespie DT. Exact stochastic simulation of coupled chemical reactions. J Phys Chem. 1977;81:2340–2361.